The Fossil Record of Cyanobacteria

2

J. William Schopf

Contents

J.W. Schopf (✉)
Department of Earth and Space Sciences, Center for the Study
of Evolution and the Origin of Life, Institute of Geophysics
and Planetary Physics, Molecular Biology Institute, University
of California, Los Angeles, CA 90095-1567, USA
e-mail: schopf@ess.ucla.edu

Abbreviations

BIF   banded iron-formation
CLSM   confocal laser scanning microscopy
GOE   Grand Oxidation Event
Ma   million years
NMR   solid-state ^{13}C nuclear magnetic resonance
RIP   Raman Index of Preservation
Rubisco   ribulose bisphospate carboxylase/oxygenase
XANES   X-ray absorption near-edge spectroscopy

Summary

Fossil evidence of cyanobacteria, represented in the geological record by microbially laminated stromatolites, cyanobacterial and cyanobacterium-like microscopic fossils, and carbon isotopic data consistent with the presence of Rubisco-mediated CO_2-fixation, extends back to ~3,500 million years ago. The most abundant and best-documented fossil cyanobacteria, known from thousands of specimens preserved in several hundred geological units, belong to five taxonomic families: the Oscillatoriaceae, Nostocaceae, Chroococcaceae, Entophysalidaceae and Pleurocapsaceae. As documented by the essentially identical morphologies, life cycles, and ecologic settings of such fossils and their modern counterparts, members of these families have exhibited extreme evolutionary stasis over enormous segments of geological time. Because of the incompleteness of the fossil record, however, such data do not resolve the time of origin of O_2-producing cyanobacteria from their anoxygenic, bacterial, evolutionary precursors. Though it is well established that Earth's ecosystem has included autotrophs since its very early stages, available data indicate only that O_2-producing photoautotrophic cyanobacteria originated earlier than the Great Oxidation Event at ~2,450 million years ago; that such microbes were evidently extant by ~2,700 million years ago; and that the origin of oxygenic photosynthesis may date from as early as, or even earlier than, 3,500 million years ago.

2.1 Overview of the Microbial Fossil Record

2.1.1 Introduction

Geological time is divided into two major segments: (1) the *Phanerozoic Eon*, the younger and much shorter of the segments, that begins with the first appearance of shelly invertebrate animals ~542 million years (Ma) ago and includes the familiar evolutionary successions from algae to spore plants and then to seed plants, and from marine invertebrates to fish and then to terrestrial vertebrates; and (2) the *Precambrian Eon*, the longer of the segments that spans the earlier seven-eighths of Earth history, extending from the formation of the planet, ~4,500 Ma ago, to the beginning of the Phanerozoic. The Precambrian, in turn, is subdivided into two exceedingly long segments – each some 2,000 Ma in duration – the *Archean*, extending from the formation of the planet to 2,500 Ma ago, and the *Proterozoic*, spanning the time from 2,500 Ma ago to the beginning of the Phanerozoic. The oldest known fossils date from ~3,500 Ma ago (Schopf 1993, 2006; Schopf et al. 2007; DeGregorio et al. 2009), with hints of life being present in ~3,830-Ma-old rocks, among the oldest known on Earth (Mojzsis et al. 1996; McKeegan et al. 2007).

Though it is likely that the earliest forms of life were heterotrophs, originating within and metabolically dependent on abiotically produced "primordial soup" (Oparin 1938; summarized in Schopf 1999), evidence from the rock record (primarily, microbially produced stromatolites, cellular microscopic fossils and the carbon isotopic composition of preserved organic matter) establishes that photoautotrophy has served as the foundation of the world's ecosystem since at least 3,500 Ma ago. The principal unsolved problem is not whether photosynthesis was an exceedingly ancient evolutionary innovation, but, rather, when did O_2-producing photosynthesis originate, a metabolic process that arose as an evolutionary derivative of a more primitive form of photoautotrophy, anoxygenic photosynthesis, characteristic of non-cyanobacterial photosynthetic bacteria (Blankenship 1992; Blankenship and Hartman 1998). Among all evolutionary innovations, the one which probably had the greatest impact on Earth's ecosystem and subsequent biotic history was the origin of O_2-producing photosynthetic cyanobacteria – dating from the earliest, Archean, segment of geological time. Their advent altered the world's environment forever and provided the biologically useable O_2 required for aerobic respiration, a decidedly more efficient energy-generating process than its anaerobic (fermentative) precursors (Schopf 1999).

The time of origin of this globally altering event can be addressed by answering a single question: "When did cyanobacteria originate?" Firm fossil evidence of the existence of cyanobacteria, the earliest-evolved "complete aerobes" capable of both O_2-producing photosynthesis and O_2-consuming respiration, would establish that the sequence of metabolic innovations that led to their emergence (anaerobic heterotrophy, followed by anaerobic photoautotrophy and then aerobic autotrophy and aerobic respiration) had already evolved, giving rise to an ancient, but metabolically fully modern, ecosystem (Schopf 1996, 1999). Evidence to answer this question should be expected to be preserved in the Precambrian rock record. Stromatolites, microbially layered deposits dominated today by filamentous and coccoid cyanobacteria, are present throughout virtually all of the known geological record; cellularly preserved fossils of cyanobacteria dominate the record of Precambrian life; and rock-derived carbon isotopic data are consistent with the presence of photosynthetic microorganisms back to ~3,500 Ma and possibly to >3,800 Ma ago. Nevertheless, a firm answer to the question of the time of origin is not yet available: the earliest known stromatolites might have been formed by anoxygenic photosynthesizers; the cyanobacterium-like fossils in rocks ~3,200- to 3,500-Ma-old might be remnants of non-O_2-producing microbes; and though a vast amount of carbon isotopic data are consistent with the presence of oxygenic photosynthesis as early as ~3,500 Ma ago, they do not rule out the possibility that the role of primary producer in the world's most ancient ecosystems was played by anaerobic, anoxygenic, photosynthetic bacteria.

It is not surprising that the question of time of origin of cyanobacteria and thus O_2-producing photosynthesis is still unresolved. In contrast to palaeontological studies of the Phanerozoic history of life, the outlines of which were already known in the mid-1800s (Darwin 1859), successful investigation of the earlier, Precambrian, fossil record did not begin until the mid-1960s (Barghoorn and Schopf 1965; Barghoorn and Tyler 1965; Cloud 1965; Schopf 1968). Although much progress has been made during the ensuing decades (e.g. Schopf and Bottjer 2009) in showing that Precambrian microbes were abundant, ubiquitous, metabolically diverse, and biotically predominant, knowledge of the early fossil record remains far from complete. Moreover, due to the "geologic cycle," the repeated sequence of mountain building, erosion, and deposition of the eroded products into sedimentary basins, the average "lifetime" of a geological unit is only some 200 Ma. For this reason, the rock record that has survived to the present rapidly diminishes with increasing geological age, which severely limits the ancient fossil record available for study. About half of the potentially fossil-bearing sedimentary rocks that have survived date from the Phanerozoic (the recent one-eighth of geological time); most of the rest are Precambrian, spanning the earlier seven-eighths of Earth history; Archean-age rocks – those older than 2,500 Ma in which evidence of the earliest oxygenic photosynthesizers is expected to occur – represent only about 5% of the surviving rock mass (Garrels and Mackenzie 1971). Although the known fossil record of cellularly preserved

microbes extends deep into the Precambrian – throughout all of the Proterozoic and much of the Archean, it becomes increasingly sparse and patchy in units older than ~2,000 Ma and the history of the various microbial lineages becomes increasingly difficult to decipher.

2.1.2 The Great Oxidation Event (GOE)

Despite the problems posed by the petering-out of the rock and fossil records over geological time, the records that *have* survived are sufficient to establish the presence of molecular oxygen in the Earth's atmosphere – and, by implication, of cyanobacterial oxygen-producing photoautotrophs – at least as early as ~2,450 Ma ago. As summarized by Holland (2002) and Canfield (2005), from about 2,200 Ma ago to the present, sandstones known as red beds have been deposited on land surfaces by meandering rivers and windblown dust. The beds are coloured red by the presence of the mineral hematite (Fe_2O_3), iron oxide that typically forms a thin veneer on individual quartz sand gains and the presence of which indicates that the atmosphere at the time was oxidizing. In contrast, in numerous terrains older than about 2,400 Ma, conglomeratic rocks occur that contain detrital grains of pyrite and uraninite deposited in shallow-water deltaic settings, minerals that in the presence of molecular oxygen are rapidly converted to their oxidized forms – for pyrite (FeS_2) to the mineral hematite (Fe_2O_3); and for uraninite (UO_2) to its soluble more-oxidized form, UO_4. If there had been appreciable oxygen in the overlying atmosphere when these shallow-water sediments were laid down, hematite, rather than pyrite, would occur in such conglomerates and uraninite would have oxidized and been dissolved.

The distinctly differing temporal distributions of red beds and of pyritic uraniferous conglomerates indicates that there was an increase in the amount of oxygen in Earth's atmosphere some 2,200–2,400 Ma ago, a date that has recently been more firmly set by studies of sulphur isotopic ratios preserved in the rock record that evidence a major rise in atmospheric O_2-content at ~2,450 Ma ago (Farquhar et al. 2000, 2007). Since photosynthesis produces well over 99% of the oxygen in the atmosphere, and since no other large-scale source of free oxygen is known, this increase of atmospheric O_2 can be firmly attributed to the activities of cyanobacterial oxygenic photosynthesizers. Nevertheless, the timing of this major increase, dubbed the Great Oxidation Event (Holland 2002), sets only a minimum age of ~2,450 Ma for the presence of these O_2-producing microbes. Because Earth's primordial environment was anoxic, the molecular oxygen generated by the earliest cyanobacteria would have been rapidly sequestered, removed from the atmosphere by its reaction with previously unoxidized substrates (e.g. volcanic gases, unoxidized minerals, and massive amounts of ferrous iron dissolved in the world's oceans) to be "sponged-up" and buried in rock-forming minerals such as the hematitic iron-oxides of banded iron-formations (BIFs) that are globally abundant in geological sequences older than 2,500 Ma. Only after all such substrates had been more or less completely oxidized – after the "rusting of the Earth" had drawn to close – could the oxygen content of Earth's atmosphere have permanently increased, a time lag from the origin of cyanobacterial O_2-producing photosynthesizers that evidently lasted for many hundreds of millions of years.

Three principal lines of evidence can be used to assess the fossil record of cyanobacteria and to address the closely related question of the time of origin of oxygenic photosynthesis – stromatolites, cellular microfossils, and the chemistry of ancient organic matter – each of which is discussed in turn below. Taken as a whole, the evidence indicates that O_2-producing cyanobacteria were extant earlier than 2,450 Ma ago; that such microbes had originated by 2,700 Ma ago; and that the origin of oxygenic photosynthesis may date from as early as, or even earlier than, 3,500 Ma ago.

2.2 Microbial Stromatolites

As preserved in the geological record, stromatolites are finely layered rock structures, typically composed of carbonate minerals (e.g. calcite, $CaCO_3$), that formed by the microbially mediated accretion of laminae, layer upon layer, from the surface of an ancient seafloor or lake bottom. Their mode of formation has been well documented by studies of modern stromatolites, structures known to microbiologists (including those specializing in studies of cyanobacteria) as "microbial mats." The layered organization of such structures reflects the photosynthetic metabolism of the mat-building and stromatolite-forming microorganisms. Thin (mm-thick) mats composed of such microbes formed as the microorganisms multiplied and spread across surfaces that were typically intermittently veneered by detrital or precipitated mineral grains that blocked sunlight. To maintain photosynthesis, mobile members of such communities, such as gliding oscillatoriacean cyanobacteria, moved upward through the accumulated mineral matter to establish a new, overlying, microbial mat. The repeated accretion and subsequent lithification of such mats, augmented commonly by an influx of non-mobile microbes (such as colonial chroococcacean, entophysalidacean, and pleurocapsacean cyanobacteria), can result in the formation of geologically preservable stromatolitic structures that range from small millimetric pustular mounds and columns to large, decimetric, bioherms. In relatively rare instances, during diagenesis (the series of changes that lead to the lithification and geological preservation of such structures), silica from ground water, precipitated as the

5 cm

1 cm

Vertically Sliced
Shark Bay
Stromatolite

20 cm

10 cm

10 cm

10 cm

10 cm
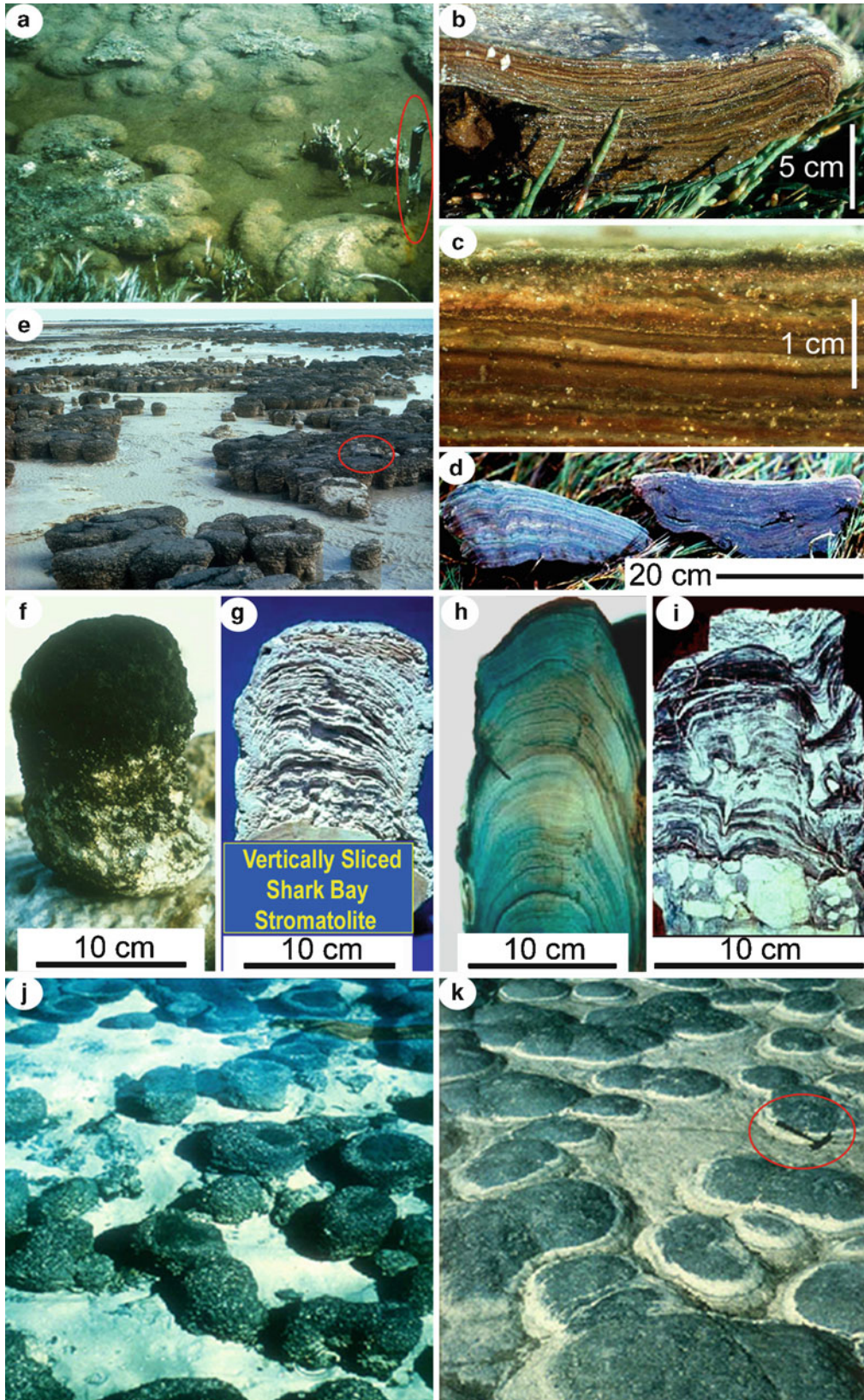
mineral quartz (SiO_2), replaces the initially formed carbonate matrix. If replacement occurs early in the history of a deposit, before the mat-building microorganisms decay and disintegrate, cellularly intact microbes can be preserved. However, the vast majority of fossil stromatolites, unaltered by such replacement, are devoid of cellularly preserved microbes: during diagenesis, carbonate grain growth crushes and obliterates the stromatolite-forming microorganisms, leaving only an amorphous thin coaly residuum of microbe-derived carbonaceous matter.

Cyanobacterium-dominated microbial mat communities, living analogues of those that produced the stromatolites of the fossil record, are known today. One such example, from Baja, Mexico, is shown in Fig. 2.1a through c and compared, in Fig. 2.1d, with a similarly laminated fossilized stromatolite ~1,300 Ma in age. Among the best known and most studied lithified modern stromatolites are those shown in Fig. 2.1e through g, carbonate microbial stromatolites that in size, shape, and laminar structure are much like those known from the Precambrian (compare Fig. 2.1g with h and i, and j and k). Such modern stromatolites are usually restricted to refugia, settings such as hot springs and hypersaline lagoons (Fig. 2.1a–g, j) in which the slow-growing microbial mats are not disrupted by grazing and burrowing metazoans. For this reason, stromatolites are not particularly abundant in sediments of the Phanerozoic, deposits laid down in environments dominated by diverse metazoans. However, in the absence of grazing and burrowing animals, as was the situation until the very end of the Precambrian, stromatolites were abundant worldwide in photic-zone carbonate-depositing settings. Known earliest from rocks ~3,500 Ma in age, their distribution over time parallels that of the surviving Precambrian rock record – that is, stromatolite-bearing rock units gradually become decreasingly abundant as the rock record gradually peters out (Fig. 2.2). Such structures establish the presence of flourishing photosynthesis-based microbial communities, but only rarely do they preserve the cellular fossils that might evidence whether the stromatolite-building photoautotrophs were oxygenic, like cyanobacteria, or anoxygenic, like photosynthetic bacteria.

2.2.1 Archean Stromatolites

As is shown in Fig. 2.2, an impressive number of Archean-age geological units – of particular interest because of their potential bearing on the time of origin of cyanobacteria – are known to contain microbially produced stromatolites. Shown in Fig. 2.3 are representative examples: carbonate sediments of the ~2,723-Ma-old Fortescue Group of Western Australia contain domical, pseudocolumnar and branching stromatolites (Fig. 2.3a, b); those of the ~2,985-Ma-old Insuzi Group of South Africa include stratiform and conical forms (Fig. 2.3c, d); and those of the ~3,388-Ma-old Strelley Pool Chert of Western Australia contain domical (Fig. 2.3e), stratiform (Fig. 2.3f) and close-packed conical stromatolites patchily distributed over many tens of square-kilometers (Fig. 2.3g–i). The presence of conical stromatolites in such deposits – like those shown in Fig. 2.3c, d, and g through i and reported from 17 of the 48 units listed in Fig. 2.2 (Hofmann et al. 1999; Hofmann 2000; Allwood et al. 2006; Schopf 2006) – is particularly noteworthy since such distinctive structures cone-shaped structures evidently require for their formation "highly motile mat builders" such as oscillatoriacean cyanobacteria (Grotzinger and Knoll 1999, pp. 342–343).

2.3 Cellular Microbial Fossils

Two principal processes preserve organic-walled cyanobacterial fossils: compression and permineralization. Compression-preserved microorganisms occur in fine-grained detrital sediments such as shales and siltstones, pressed and flattened along bedding planes as the sediment lithified. Although such carbonaceous compression-preserved microbes are poorly known from the Phanerozoic, largely neglected by Phanerozoic palaeontologists who focus chiefly on megascopic fossilized remains, they are appreciably better documented in the Precambrian (e.g. Butterfield 2009).

The microbial fossil record is best known from microorganisms preserved by permineralization. Of all modes of fossil preservation, this process (known also as petrification)

Fig. 2.1 Modern and fossil stromatolites: (a–c) Modern unlithified stromatolites (microbial mats) at Laguna Figueroa (Laguna Mormona), Baja, Mexico: (a) mound-shaped stromatolites (machete, at *right*, for scale); (b) vertically sectioned stromatolite comprised of stacked, laterally continuous, microbial mats; (c) uppermost part of the specimen in (b) showing the cyanobacterium-dominated growth surface (*green layer*, at *top*) and an immediately underlying *pinkish layer* populated by purple photosynthetic bacteria. (d) The vertically sectioned modern stromatolite in (b), at *right*, for comparison with a vertically sectioned fossil carbonate stromatolite (*left*) from the ~1,300-Ma-old Belt Supergroup of Montana, USA. (e) Modern lithified (carbonate) columnar and domical stromatolites at Shark Bay (Hamelin Pool), Western Australia (geologic hammer, at *right*, for scale), exposed at low tide. (f, g) Modern Shark Bay columnar stromatolite, in (f) showing its cyanobacterium-coated growth surface and, in a vertical section of this specimen shown in (g), its lithified, upwardly accreted, microbially produced internal layers. (h, i) For comparison with the lithified modern stromatolite in (f) and (g), vertically sectioned fossil stromatolites from the ~1,300-Ma-old Belt Supergroup of Montana, USA (h) and the ~3,350-Ma-old Fig Tree Group of the eastern Transvaal, South Africa (i). (j, k) Modern lithified Shark Bay stromatolites (j) for comparison with (k) fossil carbonate stromatolites from the ~2,300-Ma-old Transvaal Dolomite, Cape Province, South Africa; the scale for (j) and (k) is shown by the *red-circled* geological hammer in (k)

Fig. 2.2 Comparison of
temporal distribution of the 48
Archean-age stromatolite-bearing
rock units now known (●) with
that of Archean-aged rocks that
have survived to the present
(*dashed line*) (Data from
Hofmann 2000; Schopf 2006)
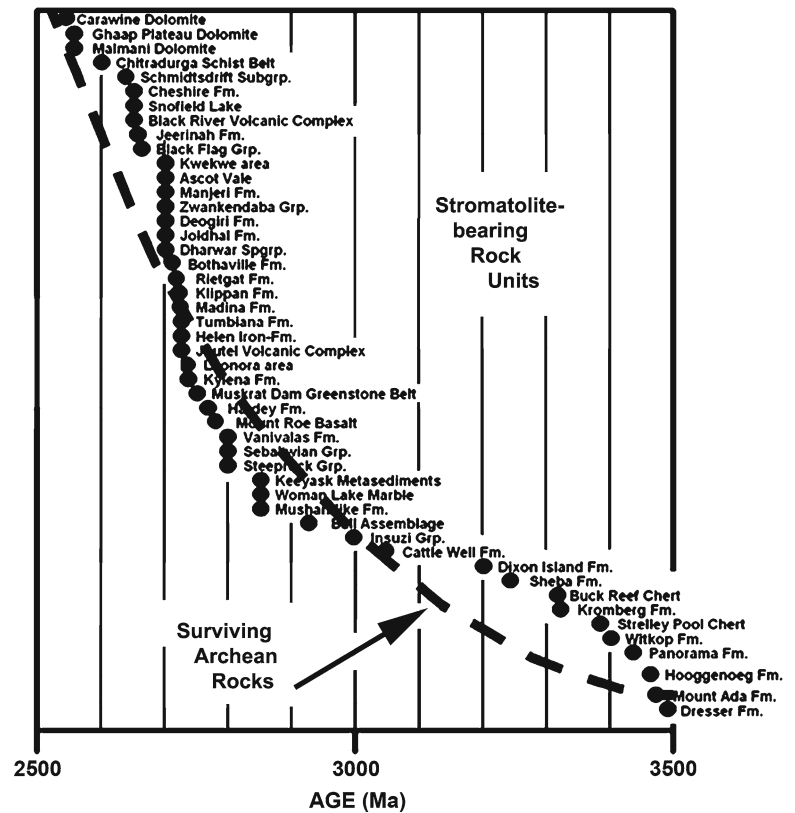
provides the most faithful representation of life-like morphology. Such preservation results from the pervasion of mineral-charged solutions into cells during the early stages of diagenesis, prior to their decay and disintegration. The permeating fluids infill microscopic voids – replacing the watery milieu of the cellular components – to produce a mineral-infused inorganic–organic mix that preserves physically robust structures such as organic-rich cell walls. As a result, both the organismal morphology and cellular anatomy of such fossils can be preserved in three-dimensional microscopic detail. The most common such permineralizing matrix is silica, fine-grained (cryptocrystalline) quartz and the mineral that comprises the rock-type known as chert. Hundreds of microbe-preserving cherts are now known from the Precambrian when silica was abundant in the world's oceans, well before the Phanerozoic appearance of silica-biomineralized sponges, diatoms and radiolarians that today regulate the oceanic silica budget. As shown here, such cherts can contain exquisitely preserved fossil microbes.

2.3.1 Modern and Fossil Cyanobacteria

Microbial classifications based primarily on biomolecular data (e.g. rRNA-, genome-, and DNA base-compositions) are for many modern microbial taxa consistent with traditional morphology-based groupings. For example, cyanobacteria have been assigned on the basis of their organismal structure and pattern of development to five "sections" (cf. morphology-defined taxonomic families) that for many genera mesh well with biochemically based classifications (Herdman et al. 1979a, b; Rippka et al. 1979). Section I (cf. Chroococcaceae) is comprised of predominantly sphe-roidal, solitary and colonial unicellular cyanobacteria that reproduce by fission or by budding (e.g. *Gloeocapsa*). Section II (cf. Pleurocapsaceae) consists of unicellular or pseudofilamentous forms that by multiple fission give rise to small daughter cells known as baeocytes (e.g. *Pleurocapsa*). Section III (cf. Oscillatoriaceae) encompasses uniseriate cyanobacterial filaments that lack cellular differentiation (e.g. *Oscillatoria* and *Spirulina*). Section IV (cf. Nostocaceae) includes simple uniseriate filaments that exhibit cellular differentiation into akinetes and heterocysts (e.g. *Nostoc*). Section V (cf. Stigonemataceae) is composed of morphologically more complex heterocystous cyanobacterial filaments that exhibit true branching. Representatives of all five groups are known from the fossil record, Sections I–IV dating from well into the Precambrian, whereas representatives of Section V are known earliest from *Stigonema*-like fossils of ~400-Ma-old Rhynie Chert of Scotland (Kidston and Lang 1922). In general, taxa included in Sections II, IV and V are consistent with biochemically-based phylogenies, whereas the cyanobacteria of Sections I and III may not comprise monophyletic lineages. However, because the biochemical
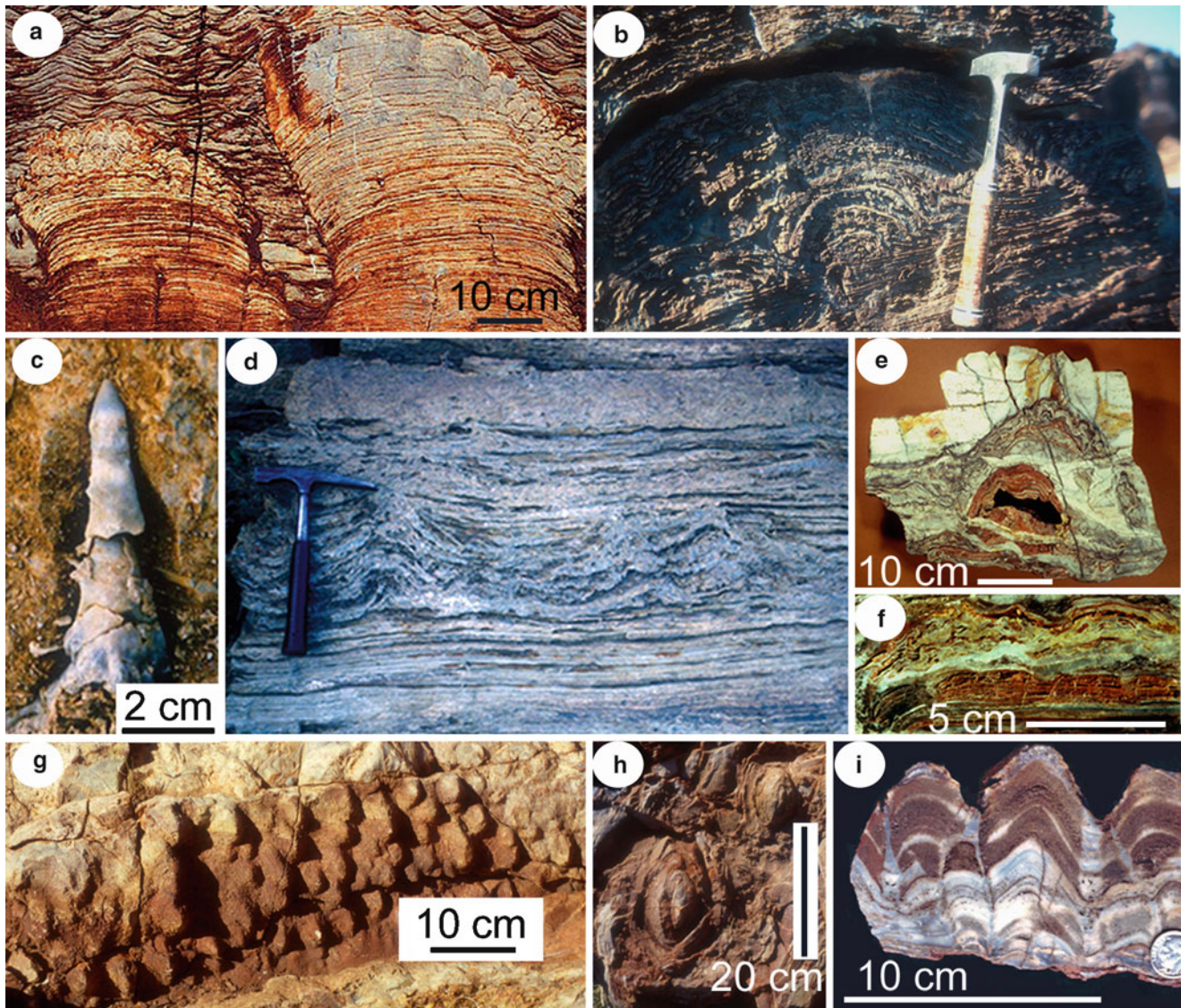
Fig. 2.3 Archean-age microbially laminated stromatolites: (**a**) Domical, pseudocolumnar and branching stromatolites, overlain by rippled sediments, and (**b**) a domical stromatolite from the ~2,723-Ma-old Tumbiana Formation (Fortescue Group) of Western Australia. (**c**) Conical stromatolite and (**d**) stratiform and conical stromatolites from the ~2,985-Ma-old Insuzi Group, South Africa. (**e–i**) Domical (**e**), stratiform (**f**), and laterally linked conical stromatolites (**g** through **i**) from the ~3,388-Ma-old Strelley Pool Chert of Western Australia

components of such microbes, like those of all living systems, are geochemically labile – converted over geological time to coaly kerogen, a geochemically stable complex mix of interlinked polycyclic aromatic hydrocarbons – the classification of cyanobacterial fossils is necessarily based on their morphology, not on their original biochemistry.

2.3.2 Identification of the Major Fossil Types

Four major categories of prokaryotic microbes are known from the fossil record: (1) cyanobacteria; (2) prokaryotes of uncertain systematic relations; (3) sulphate-reducing bacteria; and (4) methane-producing archaeans. Of these, the fossils of uncertain relations (viz., Prokaryotes *Incertae Sedis*) are all regarded as members of the Bacterial rather than the Archaeal Domain, the uncertainty of their systematic position reflecting their morphological similarity both to cyanobacteria and to members of noncyanobacterial bacterial groups. The sulphate-reducers and the methane-producers are known only from isotopic evidence, not from morphologically preserved cellular fossils. Of the four categories, cyanobacteria have the best-documented fossil record, known from thousands of specimens cellularly preserved in hundreds of geological units. Many such fossils are indistinguishable from members of extant cyanobacterial taxa, not only in their morphology

and cellular structure but also in their life cycles and inferred processes of cell division as well as their ecological setting, the biotic structure of the communities in which they occur, and the types of stromatolites they produce.

In comparison with other prokaryotes, whether bacterial or archaeal, most cyanobacteria have somewhat larger cells and more complex morphology. Because of their light-requiring photosynthetic metabolism, cyanobacteria occupy the uppermost surface of microbial mats, rather than lower regions of such biocoenoses where decay and cellular disintegration are prevalent. For this reason, cyanobacteria have a higher probability of becoming incorporated in the fossil record as cellularly intact specimens than do other prokaryotes, especially if they are preserved by permineralization during the early stages of sediment lithification. Of the various morphological components of cyanobacteria, extracellular sheaths and envelopes, initially composed largely of carbohydrates and relatively resistant to degradation, are the most commonly preserved. Although physically robust and organic-rich, cell walls are somewhat less commonly preserved, and in the cells of fossilized cyanobacterial filaments, the originally peptidoglycan-containing thick lateral walls are more commonly preserved than the thinner peptidoglycan-deficient transverse walls. The intracellular biochemical and structural components of such cells (e.g. ribosomes, proteins, strands of DNA, RNA and the like) are evidently never preserved intact. Not only are such components geochemically unstable (degrading to their monomeric constituents within a few to tens of thousands of years), but also, along with the watery intracellular milieu, such organics are typically leached out of such cells during preservation or, if recombined into kerogen,

occur as constituents of small coaly carbonaceous intracellular bodies, collapsed remnants of degraded protoplasm.

2.4 Cyanobacterial Fossils

The fossil record of cyanobacteria, summarized here based on specimens preserved in Precambrian-age deposits where the group is well-known and best documented, is composed primarily of oscillatoriacean and nostocacean filaments and of chroococcacean, entophysalidacean and pleurocapsacean coccoid to ellipsoid unicells and colonies. Members of these five cyanobacterial families – each of which is discussed, in turn, below – are the principal components also of modern mat-building microbial stromatolitic communities.

2.4.1 Filamentous Cyanobacteria

2.4.1.1 Oscillatoriaceae

Among the five families of cyanobacteria that are well represented in the fossil record, the Oscillatoriaceae, cyanobacteria characterized by simple unbranched uniseriate trichomes composed of discoidal, equant, or elongate cells, has the most extensive record, represented by diverse fossils in hundreds of ancient microbial communities. Representative Precambrian examples (~775- to ~800-Ma in age) are shown in Fig. 2.4b d, through f, compared with modern morphological analogues (Fig. 2.4a, c). Although the trichomes of many extant oscillatoriaceans maintain a uniform diameter throughout their length (e.g. Fig. 2.4a, i, n, o), some typically

Fig. 2.4 **Modern and fossil oscillatoriacean cyanobacteria:** Fossil specimens are in petrographic thin sections of stromatolitic cherts from the ~800-Ma-old Bitter Springs Formation of central Australia (**b**, **d**, **g**, **h**, **aa** and **bb**) and the ~775-Ma-old Chichkan Formation of southern Kazakhstan (**e**, **f**, **k** through **m**, and **p** through **x**), and in acid-macerates of siltstones from the ~1,020-Ma-old Lakhanda Formation (**j**) and ~850-Ma-old Miroedikha Formation (**z**), both of Siberia, Russia. (**a**, **b**) Optical images of modern *Oscillatoria* sp. (**a**) and the morphologically similar fossil *Oscillatoriopsis breviconvexa* (**b**). (**c**, **d**) Optical images of modern *Oscillatoria amoena* (**c**) and its fossil counterpart, *Cephalophytarion grande*. (**e**, **f**) Optical montage (**e**), composed of six micrographs (denoted by the *white lines*) and, in (**d**), a confocal laser scanning microscopy (*CLSM*) image of fossil *Oscillatoriopsis* sp. showing its discoidal medial cells. (**g**, **h**) Optical montage (**g**), composed of ten photomicrographs (denoted by the *white lines*) and a CLSM image (**h**) of a cellular trichome (*Cephalophytarion laticellulosum*) that descends from where it transects the upper surface of the thin section (at the *far right*) to a depth of 20 μm (at the *far left*). (**i**, **j**) Optical images of modern *Lyngbya* sp. and its fossil counterpart, *Paleolyngbya helva; arrows* point to trichome-encompassing tubular organic sheaths. (**k–m**) Optical (**k** and **l**) and a CLSM image (**m**) of *Siphonophycus solidum*, the extracellular tubular sheath of an oscillatoriacean cyanobacterium, the *red rectangle* in (**k**) denoting the area imaged in (**l**) and (**m**). (**n**, **o**) Optical images of two specimens of modern *Oscillatoria* sp. showing the rounded terminal cells (*left*), disc-shaped medial cells, and partial septations

(*arrows*) characteristic of oscillatoriacean cyanobacteria. (**p**) Optical image of fossil *Oscillatoriopsis media* descending into a thin section at a low angle from *left* to *right*, shown in a photomontage in which the *red rectangles* denote the areas of the trichome shown in CLSM images (**q** through **u**) and three-dimensional Raman images (**v** through **x**). (**q**) The trichome terminus, showing its rounded end-cell and subtending disc-shaped medial cells. (**r**) Part of the trichome situated ~14 μm deeper in the section than the trichome terminus (and ~28 μm below the upper surface of the section) that exhibits partial septations (*arrows*) like those shown in (**n**) and (**o**). (**s–u**) A deeper part of the trichome (~39 μm below upper surface of section) that similarly exhibits partial septations (*arrows*), in (**s**) and (**t**) showing the specimen as viewed from above its upper surface [the same perspective as shown in (**p**), but in (**t**) with the trichome tilted slightly to the right to show its interior], and in (**u**) showing the trichome as viewed from its side. (**v–x**) Three-dimensional Raman images (acquired in a spectral window centered in the kerogen "G" band at ~1,605 cm^{-1}) showing the kerogenous composition of the trichome and its partial septations: (**v**), the part of specimen denoted by the *red rectangle* in (**s**), as viewed from above the trichome; (**w**), the part denoted in (**t**), titled slightly to the *left*; (**x**), the part denoted in (**u**), showing the specimen from its side. (**y–bb**) Optical photomicrographs (**y** through **aa**) and a CLSM image (**bb**) showing modern *Spirulina* (**a**) for comparison with its helically coiled fossil counterparts, a *Spirulina*-like trichome in (**z**) and, in (**aa**) and (**bb**), *Heliconema funiculum*, in (**aa**) shown in montage composed of five photomicrographs (denoted by *white lines*)
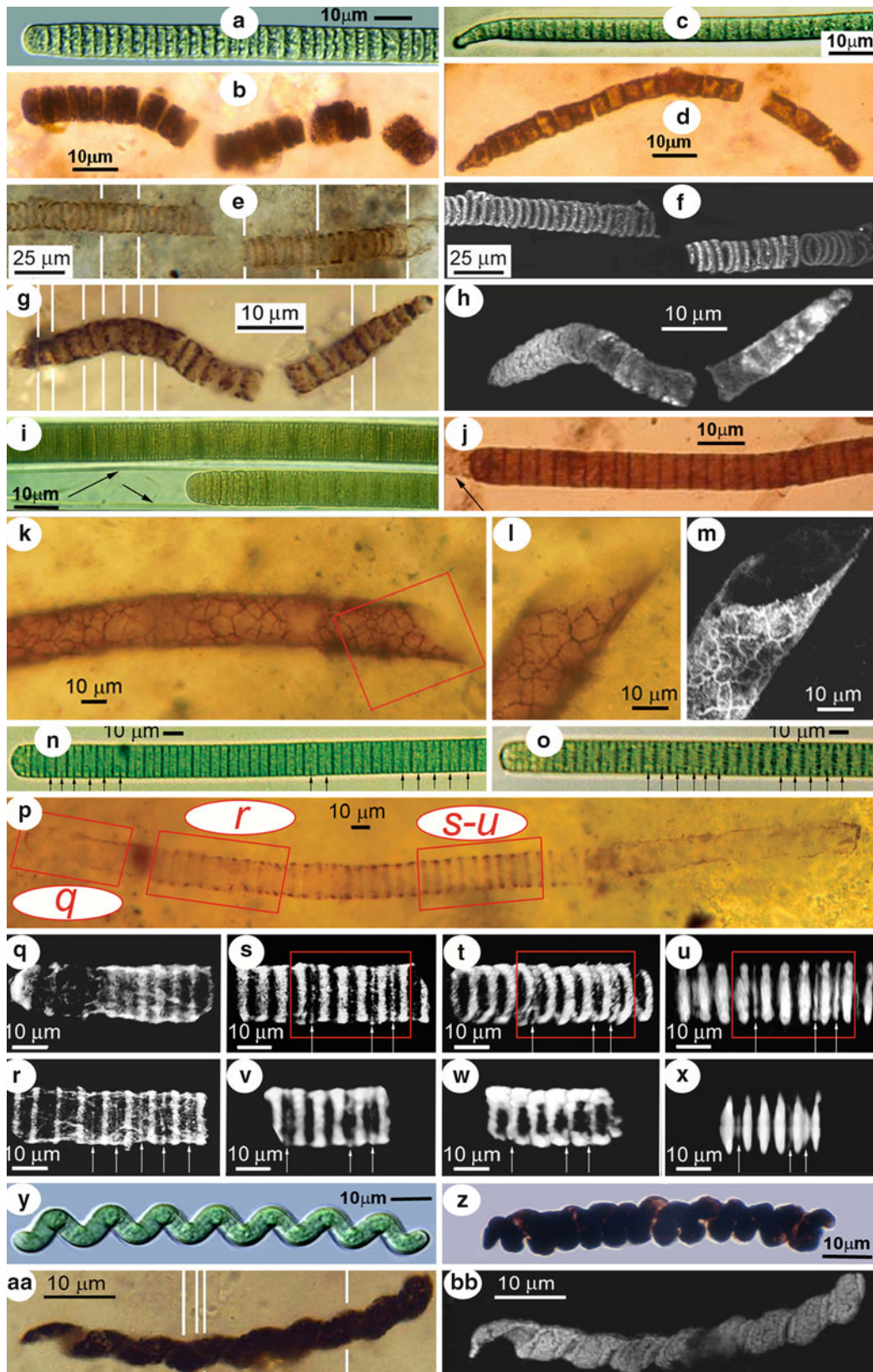
taper toward their apices (Fig. 2.4c), tapered trichomes that are also recorded in fossil examples (Fig. 2.4d, g, h). In addition, although many modern oscillatoriacean trichomes lack (or are enclosed by a very thin) extracellular tubular sheath (e.g. *Oscillatoria*: Fig. 2.4a, c, n, o), others, such as *Lyngbya* are encompassed by a prominent mucilaginous sheath (Fig. 2.4i) which, like the cell walls of oscillatoriacean trichomes, can be preserved in fossil specimens (Fig. 2.4j–m).

The trichomes of the great majority of members of the Oscillatoriaceae are characterized by rounded terminal cells, disc-shaped medial cells, and partial septations, incipient cell walls that grow inward to produce daughter cells (arrows in Fig. 2.4n, o). Although in fossil specimens such thin incipient cell walls are rarely evident by optical microscopy, two techniques recently introduced to such studies (Schopf and Kudryavtsev 2005; Schopf et al. 2002, 2005, 2006) – confocal laser scanning microscopy (CLSM) and Raman imagery – can be used to establish their presence. For example, compare the photomicrographs of modern *Oscillatoria* (Fig. 2.4n, o) with that of its fossil equivalent, *Oscillatoriopsis media*, shown in Fig. 2.4p in a thin slice of chert (a ~100-µm-thick petrographic thin section) from the ~775-Ma-old Chichkan Formation of southern Kazakhstan. Because of the CLSM detectable laser-induced fluorescence of the coaly kerogen (primarily, interlinked polycyclic aromatic hydrocarbons) that comprises the cell walls of the fossil, its detailed cellular structure is appreciably better defined in the CLSM images (Fig. 2.4q–u) than in the corresponding optical image (Fig. 2.4p), whereas 3-D Raman imagery documents the carbonaceous composition of its permineralized (quartz-infused) cells (Fig. 2.4v–x).

The cells of modern oscillatoriaceans divide by the centripetal invagination of partial septations that fuse in the center of a cell to produce transverse cell walls. The lateral cell walls of such trichomes are about twice the thickness of their transverse walls and they contain rigidifying pepdidoglycans that are absent from partial septations and transverse walls except at the cell periphery (Pankratz and Bowen 1963; Frank et al. 1971; Halfen and Castenholz 1971; Drews 1973). Because of these differences, lateral cell walls tend to be relatively well preserved in fossil specimens whereas the thinner transverse walls, like their precursor partial septations, are typically preserved only in part. Despite these differences, use of CLSM to analyze fossil specimens shows the presence of such partial septations (arrows in Fig. 2.4r–u), with 3-D Raman imagery (Fig. 2.4v–u) confirming their carbonaceous composition. Not only do such data establish the oscillatoriacean affinities of such fossil cellular trichomes, showing that they are morphologically essentially identical to living members of the family, but they indicate also that their cell division occurred by the same genetically determined processes as their modern counterparts. Data such as these show that the fossil record of the Oscillatoriaceae

extends deep into geological time and that such cyanobacteria have changed little or not at all over thousands of millions of years (Schopf 1994a, 1999, 2009).

In addition to cellular (e.g. *Oscillatoria*) and prominently ensheathed trichomes (e.g. *Lyngbya*), the Oscillatoriaceae includes distinctive spirally wound filaments such as the modern *Spirulina* shown in Fig. 2.4y. As shown in Fig. 2.4z through bb, such *Spirulina*-like helically coiled filaments are known also from the Precambrian fossil record.

2.4.1.2 Nostocaceae

In comparison with the fossil record of oscillatoriaceans, that of similarly filament-forming nostocaceans is poorly known. A characteristic of the Nostocaceae is the presence of intercalary heterocysts, thick-walled cells that permit the nitrogenase enzyme complex of filaments living in a well-oxygenated environment to fix N_2, and which only develop when the organism is deprived of other usable N sources (Schopf 1978). As bacterially generated ammonia is plentiful in stromatolitic microbial communities, neither fossil nor modern filamentous cyanobacteria in them are heterocystous. Such differentiated cells being first known from the Devonian Rhynie chert (Kidston and Lang 1922). Nevertheless, based on organismal and cellular morphology, numerous Precambrian fossils have been assigned to the Nostocaceae. Two such examples are shown in Fig. 2.5b, c, compared with modern *Nostoc* (Fig. 2.5a). Nostocaceans are also represented in the Precambrian record by elongate spore-like cells such as *Archaeoellipsoides* (Horodyski and Donaldson 1980) that date back to ~2,100 Ma ago and closely resemble the reproductive akinetes of extant members of the family (Golubić et al. 1995). One such fossil (*Archaeoellipsoides longus*) is shown in Fig. 2.5d through f. The temporal distribution of the Nostocaceae fits well with the timing of the Great Oxidation Event, ~2,400 Ma ago, before which the nitrogenase-protecting heterocysts of akinete-producing nostocaceans would have been of little selective advantage. Further, rRNA phylogenies indicate that the Nostocaceae, like other heterocystous cyanobacterial families, originated in a burst of evolution well after the appearance of families composed of non-heterocystous coccoid, ellipsoid and filamentous taxa (Giovannoni et al. 1988; Zehr et al. 1997). Like other cyanobacteria, nostocaceans appear to have evolved little or not at all since their origination more than 2,000 million years ago (e.g. compare Fig. 2.5a with b and c).

2.4.2 Coccoid and Ellipsoid Cyanobacteria

2.4.2.1 Chroococcaceae

Figure 2.6 shows numerous specimens of fossil chroococcaceans, characterized by their typical occurrence in envelope-
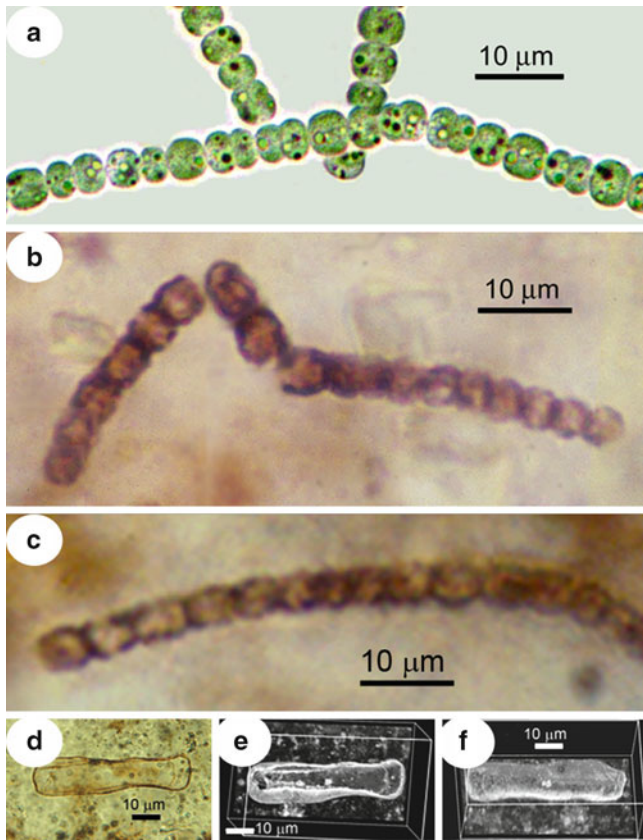
Fig. 2.5 **Modern and fossil nostocacean cyanobacteria**: (**a**) Modern *Nostoc* PCC 7936 for comparison with two specimens of *Veteronostocale amoenum* (**b**, **c**) shown in a petrographic thin section of stromatolitic chert from the ~800-Ma-old Bitter Springs Formation of central Australia. (**d**–**f**) *Archaeoellipsoides longus*, ankinete characteristic of nostocacean cyanobacteria, from a thin section of the ~775-Ma-old Chichkan Formation of southern Kazakhstan, shown in an optical photomicrograph (**d**) and in (**e**) and (**f**), in confocal laser scanning micrographs: in (**e**), from above the specimen, the same perspective as in (**d**); in (**f**), from below the specimen, showing its smooth lower side

enclosed colonies composed of a few to many coccoid cells. Although chroococceans are usually major components of stromatolitic communities, they are almost always of lesser abundance than filamentous mat-building cyanobacteria. Fossils referred to the Chroococcaceae range from isolated single cells, not uncommonly enveloped by multilamellated sheaths (Fig. 2.6a), to pairs (Fig. 2.6b, c) or quartets of sheath-enveloped (Fig. 2.6d–h) or sheath-lacking (Fig. 2.6k–s) spheroidal cells. Some such specimens exhibit a flat-sided "lima bean-shape" (Fig. 2.6b, c, h, p–s) that evidences their formation by cell division like that of modern chroococceans, whereas others occur in large aggregates of geometrically ordered (Fig. 2.6i) or irregularly distributed (Fig. 2.6j, t, u) close-packed colonial cells. As shown in Fig. 2.6o, r, s, studies by CLSM provide high-resolution three-dimensional images of such rock-embedded fossils unavailable from standard photomicrography. Virtually all fossil chroococceans

are similar in salient characteristics (e.g. cell size, cell shape, ensheathed habit, colonial organization, environmental setting) to extant members of the family (compare, for example, Fig. 2.6g, h).

2.4.2.2 Entophysalidaceae

Other fossil cyanobacteria, typically occurring in globose to pustular colonies composed of large numbers of small ellipsoid cells and known from deposits as old as ~2,600 Ma (Altermann and Schopf 1995), are notably similar to modern members of the cyanobacterial family Entophysalidaceae. A rather typical example is shown in Fig. 2.7b, a part of a colony of fossil *Eoentophysalis belcherensis* (Hofmann 1976) preserved in stromatolitic chert of the ~2,100-Ma-old Kasegalik Formation of Canada, compared with living *Entophysalis* (Fig. 2.7a) present in a modern stromatolitic microbial mat community. The similarities between such modern and fossil cyanobacteria are striking: not only are the fossil and modern species morphologically indistinguishable (in cell shape, and in the form and arrangement of originally mucilaginous cell-encompassing envelopes), but they exhibit similar frequency distributions of dividing cells and essentially identical patterns of cell development (resulting from cell division in three perpendicular planes); they form microtexturally similar stromatolitic structures in comparable intertidal to shallow marine environmental settings; they undergo essentially identical postmortem degradation sequences; and they occur in comparable microbial communities, similar both in species composition and in overall diversity (Golubić and Hofmann 1976). Moreover, both in modern and in fossil stromatolites, such entophysalidaceans can be sufficiently abundant to be important mat-formers as shown for a fossil in Fig. 2.7c, stromatolitic layers formed by laterally linked colonies of *Eoentophysalsis* in Kasegalik Formation stromatolites.

2.4.2.3 Pleurocapsaceae

Like entophysalidaceans, baeocyte-producing pleurocapasacean cyanobacteria have an ancient fossil record (Zhang and Golubić 1987). Shown in Fig. 2.8b, for example, is a part of a colony of the Precambrian pleurocapsacean *Paleopleurocapsa reniforma* compared with modern *Pleurocapsa* sp., its living morphological counterpart (Fig. 2.8a). Such fossil and living pleurocapsaceans can be compared in detail. The most studied such example, *Polybessurus bipartitus*, first reported from ~775-Ma-old stromatolites of South Australia (Fairchild 1975; Schopf 1977), is a morphologically distinctive cylindrical fossil pleurocapsacean composed of nested cup-shaped envelopes that extend into long tubular stalks oriented perpendicular to the substrate (Fig. 2.8c–h). Specimens of this taxon in rocks of about the same age from East Greenland have been described as being "a close morphological, reproductive, and behavioral counterpart" to the modern
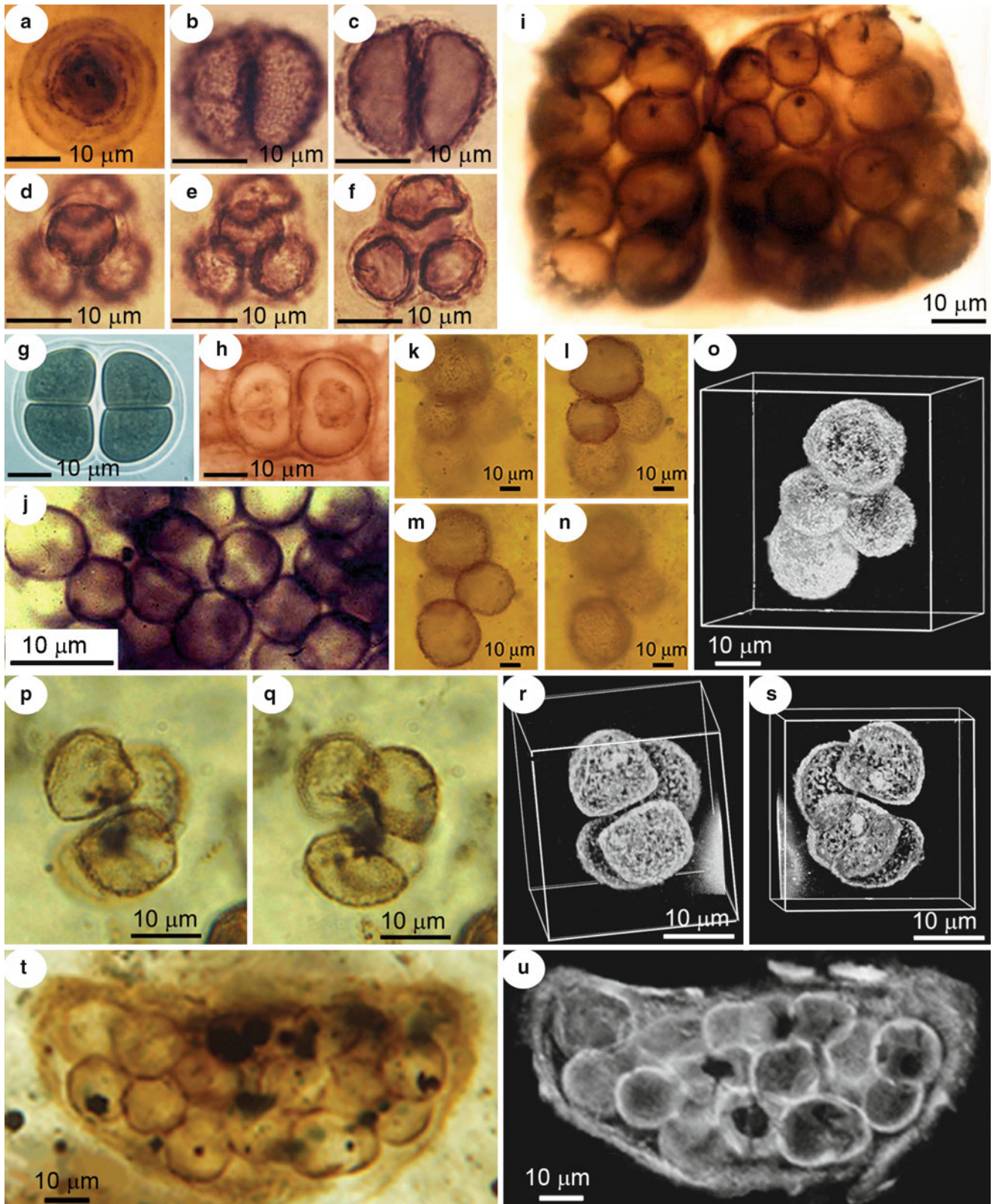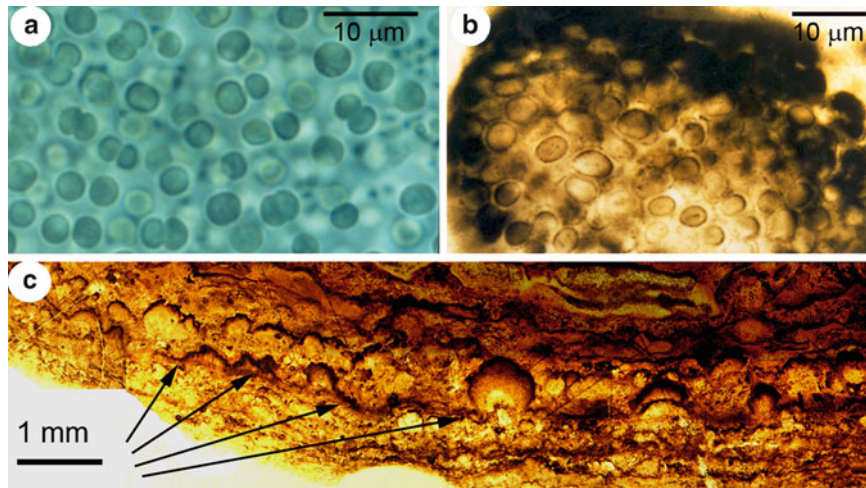
Fig. 2.7 Modern and fossil entophysalidacean cyanobacteria: (**a**) Modern *Entophysalis* sp. for comparison with (**b**) *Eoentophysalis belcherenisis*, in a petrographic thin section of stromatolitic chert of the ~2,100-Ma-old Kasegalik Formation from the Belcher Islands, Canada. (**c**) Low-magnification optical image of pustular stromatolitic laminae formed by laterally interlinked (at *arrows*) entophysalidacean colonies in these stromatolitic cherts

pleurocapsacean *Cyanostylon* present "in Bahamian environments similar to those in which the Proterozoic fossils occur" (Green et al. 1987, p. 928). Another fossil pleurocapsacean (*Palaeopleurocapsa wopfnerii*), described from the ~770-Ma-old Skillogalee Formation of South Australia, has been compared with its living morphological and ecological analogue (*Pleurocapsa fuliginosa*) and interpreted as "further evidence of the evolutionary conservatism of [cyanobacteria]" (Knoll et al. 1975, p. 2492). Two other species of morphologically distinct fossil pleurocapsaceans (the endolithic *Eohyella dichotoma* and *E. rectroclada*), regarded as "compelling examples of the close resemblance between Proterozoic prokaryotes and their modern counterparts" (Knoll et al. 1986, p. 857), have been described from the East Greenland geologic sequence as being "morphologically, developmentally, and behaviorally indistinguishable" from living *Hyella* of the Bahama Banks (Green et al. 1988, pp. 837–838).

2.4.3 Synopsis

Given the foregoing, it is well established that:

- the fossil record of the cyanobacterial lineage extends deep into geological time, to earlier than the GOE at ~2,450 Ma;
- this record, based on thousands of fossils from hundreds of geological units, is particularly well documented for five cyanobacterial families: the Oscillatoriaceae, Nostocaceae, Chroococcaceae, Entophysalidaceae, and Pleurocapsaceae; and
- many members of these families have evidently evolved little or not at all over thousands of millions of years.

One major question has yet to be resolved, namely, When did O_2-producing cyanobacteria first emerge? Evidence from Archean-age (>2,500-Ma-old) rocks may hold the answer. Two key lines of evidence must be considered: (1) the Archean record of microbial fossils and (2) the organic geochemical evidence of ancient microbes preserved in such ancient rocks. Each of these is addressed below.

◄

Fig. 2.6 Modern and fossil chroococcacean cyanobacteria: Fossil specimens are in petrographic thin sections of stromatolitic cherts from the ~1,000-Ma-old Sukhaya Tunguska Formation of Siberia, Russia (**a** and **i**), the ~800-Ma-old Bitter Springs Formation of central Australia (**b** through **f** and **j**), the ~1,500-Ma-old Satka Formation of Bashkiria, Russia (**h**), and the ~775-Ma-old Chichkan Formation of Siberia, Russia (**k** through **u**). (**a–h**) Sheath-enclosed *Gloeocapsa*-like cyanobacteria, spanning a range of morphologies from a multilamellated single cell (**a**), to a sheath-enveloped cell-pair (**b** and **c**), to four-celled sheath-enclosed colonies (**d** through **h**) that illustrate the similarity of modern *Gloeocapsa* sp. (**g**) and its fossil counterpart (*Gloeodiniopsis uralicus*, shown in **h**). (**i**, **j**) Many-celled colonies of fossil chroococcaceans. (**k–o**) 4-celled colony of fossil chroococcaceans showing that, in comparison with optical images obtained at sequentially increasing focal depths (**k** through **n**), appreciably more information can be provided by a single confocal laser scanning microscope (CLSM) image (**o**). (**p–s**) Optical (**p** and **q**) and CLSM (**r** and **s**) images of a four-celled fossil chroococcacean colony of decussate cells (*Myxococcoides dilutus*): (**p**), upper cell pair; (**q**), lower cell pair; (**r**), CLSM image from the perspective shown in (**p**) and (**q**); (**s**), the image shown in (**r**) rotated to show the underside of the decussate tetrad. (**t**, **u**) Optical (**t**) and CLSM (**u**) images of a many-celled fossil chroococcacean (*Myxococcoides inornata*) enveloped by a diaphanous sheath

Fig. 2.8 Modern and fossil pleurocapsacean cyanobacteria:
(**a**) Modern *Pleurocapsa* sp. (PCC 7327) for comparison with (**b**) *Paleopleurocapsa reniforma* in a petrographic thin section of stromatolitic chert from the ~775-Ma-old Chichkan Formation of southern Kazakhstan. (**c–h**) Specimens of the colonial stalk-forming pleurocapsacean cyanobacterium *Polybessurus bipartitus* in petrographic thin sections of stromatolitic chert from the ~775-Ma-old River Wakefield Formation of South Australia: longitudinal (**c**) and transverse sections (**d**) of a colony of pincushion-like vertically oriented and originally mucilaginous extracellular stalks; (**e**) a multilamellated ellipsoid cell at the upper end of a stalk; (**f** and **g**) longitudinal sections of asymmetrically laminated mucilaginous stalks, in (**f**) capped by the ellipsoid stalk-forming cell; (**h**) interpretive drawings (based on tracings of photomicrographs) showing from (*1*) through (*4*) the ontogeny of stalk-formation
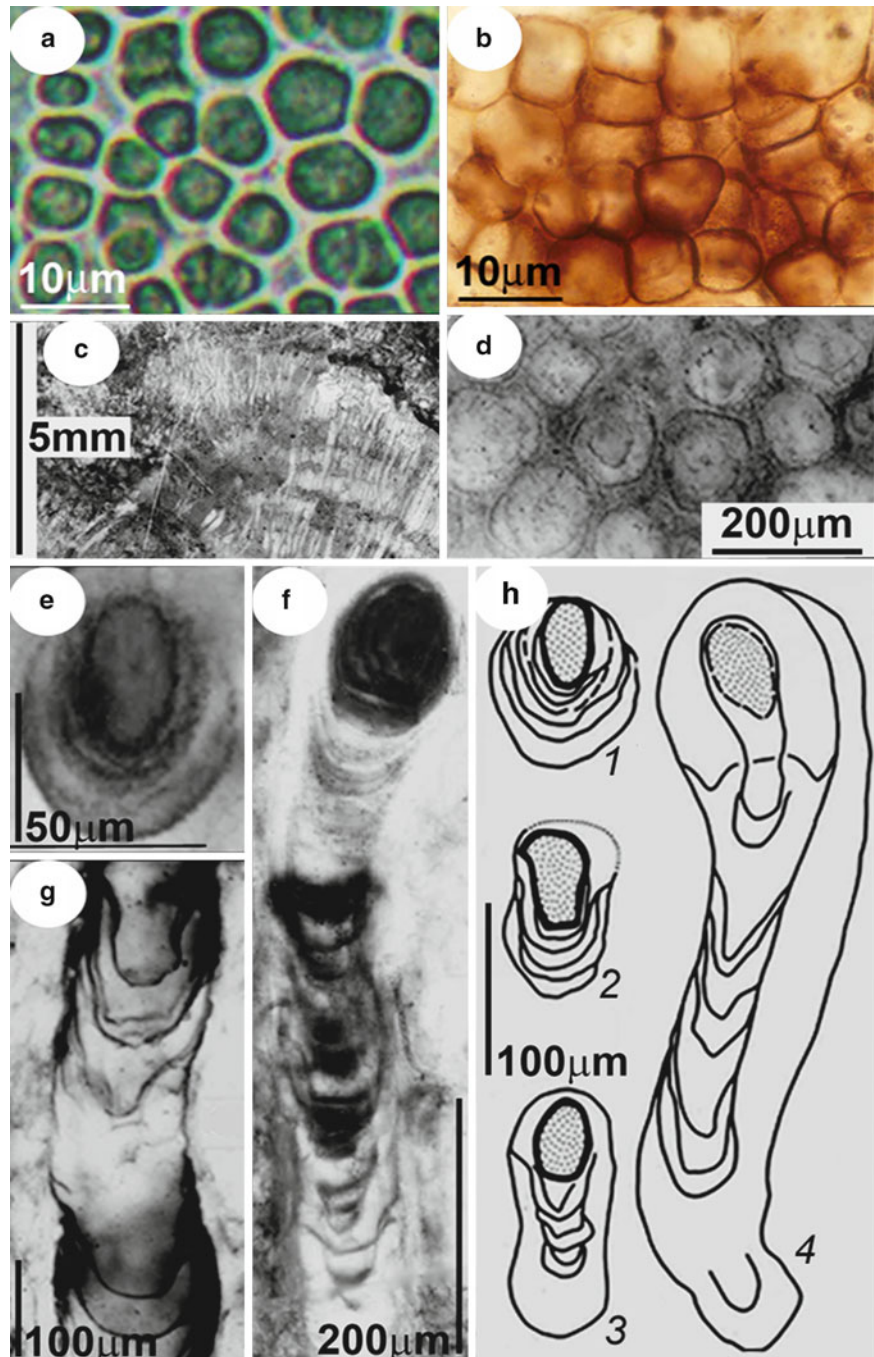
2.5   Archean Microbial Fossils

Although cyanobacteria are certain to have been extant by 2,450 Ma ago, and though the O_2-producing photosynthesis that characterizes the group must have originated appreciably earlier, exactly how much earlier remains to be established. Is this uncertainty due to the petering-out over time of the rock record (and the fossil-destroying metamorphic alteration to which the older surviving rocks have been subjected), or, rather, does the fossil record, as now known, evidence the true evolutionary history of the cyanobacterial lineage?

Fossils classed as Bacteria *Incertae Sedis* – that is, fossil prokaryotes of the Bacterial Domain that cannot be referred with certainty to a particular bacterial group – are known throughout the geological record. For virtually all such fossils, the uncertainty in their classification stems from their morphological similarity both to cyanobacteria and to noncyanobacterial bacteria. Such remnants constitute the great majority of

the fossils now known from Archean-age rocks. Because of geologic recycling, only about 5% of rocks exposed at the Earth's surface date from the Archean (Garrels and Mackenzie 1971). Not surprisingly, therefore, the record of Archean microbial fossils is sparse, in the interval between 2,500 and 3,500 Ma reported from only some 40 rock units and comprising only six broad bacterium-like morphotypes (Schopf 2006). Nevertheless, of these geological units, 14 date from the interval between 3,200 and 3,500 million years ago, well evidencing the presence of microbe-level life this early in Earth history.

The Archean fossil microbes most studied are those of the ~3,465-Ma-old Apex chert of northwestern, Western Australia (Schopf 1992a, 1993, 1999; Schopf et al. 2002, 2007). Shown in Fig. 2.9. are specimens of *Primaevifilum conicoterminatum* (Fig. 2.9a, b) and *P. amoenum* (Fig. 2.9c–m), two of 11 taxa of filamentous microorganisms described from this unit (Schopf 1993). These distinctly cellular microscopic fossils, and many of the nine other taxa reported from the deposit, are "cyanobacterium-like" in their morphology and cellular anatomy (e.g. compare Fig. 2.9c–g with Fig. 2.4b, d, g). Nevertheless, because of microbial mimicry – the occurrence of more or less identical morphologies in taxa of oxygenic and non-oxygen-producing microbes (Schopf 1992b, 1999) – organismal and cellular morphology, in and of themselves, cannot provide firm evidence of the physiological capabilities of such very ancient microbes (Schopf 1993). This uncertainty could be resolved were the Archean fossil record, like that of the Proterozoic, sufficiently continuous and well-documented to unambiguously link younger fossils of well-established affinities to their older, and typically less well preserved, evolutionary precursors.

2.6 Organic Geochemical Evidence of Archean Microbes

The existence both of microbially laminated stromatolites and of "cyanobacterium-like" microscopic fossils in rocks dating from ~3,500 Ma ago suggests – but does not establish – that cyanobacteria were extant at this very early stage in Earth history. Rather, such stromatolites and fossils might actually evidence the presence of non-O_2-producing photosynthetic bacteria, evolutionary precursors of the cyanobacterial lineage. In an effort to resolve this question, we will now turn to the data provided by the chemistry of preserved Archean organic matter.

2.6.1 Hydrocarbon Biomarkers

Extraction, isolation, and identification by gas chromatography-mass spectroscopy of organic biomarkers, particularly of various types of hydrocarbons, have provided useful insight into the nature of Precambrian life. For example, identification of the protozoan biomarker tetrahymenol in ~930-Ma-old sediments of the Grand Canyon, Arizona (Summons 1992), supported by the presence of fossils of testate amoebae in the same sedimentary sequence (Bloeser et al. 1977; Bloeser 1985; Schopf 1992c; Porter and Knoll 2000), has established a minimum age for the Proterozoic origin of protozoan protists.

In general, however, such studies have not proven useful to Archean-age deposits. Among the most promising of the few such reports is that of steranes (hydrogenated derivatives of steroids, such as cholesterol) identified in extracts of ~2,700-Ma-old carbonaceous shales of northwestern Australia (Brocks et al. 1999). This finding is unexpected, since steroids occur almost exclusively in eukaryotic cells (e.g. Summons et al. 2006), principally as the components of intracellular membranes, and assured fossil eukaryotes (relatively large-celled spheroidal phytoplankton) are known earliest from sediments ~1,800 Ma in age (Schopf 1992c) that are nearly a billion years younger than the sterane-containing rocks. However, if the reported steranes date from ~2,700 Ma ago, their occurrence would seem to indicate that biologically produced molecular oxygen must have been present in the local environment: steroid biosynthesis involves numerous O_2-requiring enzyme-mediated steps (for cholesterol, 11 such steps, beginning with the cyclization of squalene: Schopf 1978; Summons et al. 2006), and the presence of ~2,700-Ma-old steranes would therefore imply that O_2-producing photosynthesizers must also have been present, since there is no other plausible source for production of the free oxygen required for steroid synthesis.

The interpretation of these reported biomarkers is complicated. Although it seems clear that the sterane-containing shales have been dated correctly, potential contamination from modern sources (e.g. from drilling fluids or introduced during laboratory analyses) is an ever-present problem in such studies. All organic compounds are soluble to some extent in ground water and for this reason can be introduced into rocks long after their deposition, from not only modern but also geologically ancient sources. Moreover, because there are no techniques by which to determine directly the age of organic compounds extracted from ancient sediments, it is difficult to show definitively that such organics are syngenetic with the rock in which they occur. Because of these and related problems, Rasmussen et al. (2008) suggested that the Australian shale-associated steranes are much younger than ~2,700 Ma, most probably less than ~2,200 Ma in age. However, subsequent, more detailed studies that correlate the distribution of these biomarkers with their carbon isotopic compositions and their differing paleoecologic settings provide convincing evidence that they are syngenetic with rocks from which they have been reported (Eigenbrode et al. 2008). And these results showing the syngenicity of such biomarkers with their enclosing sediments have even
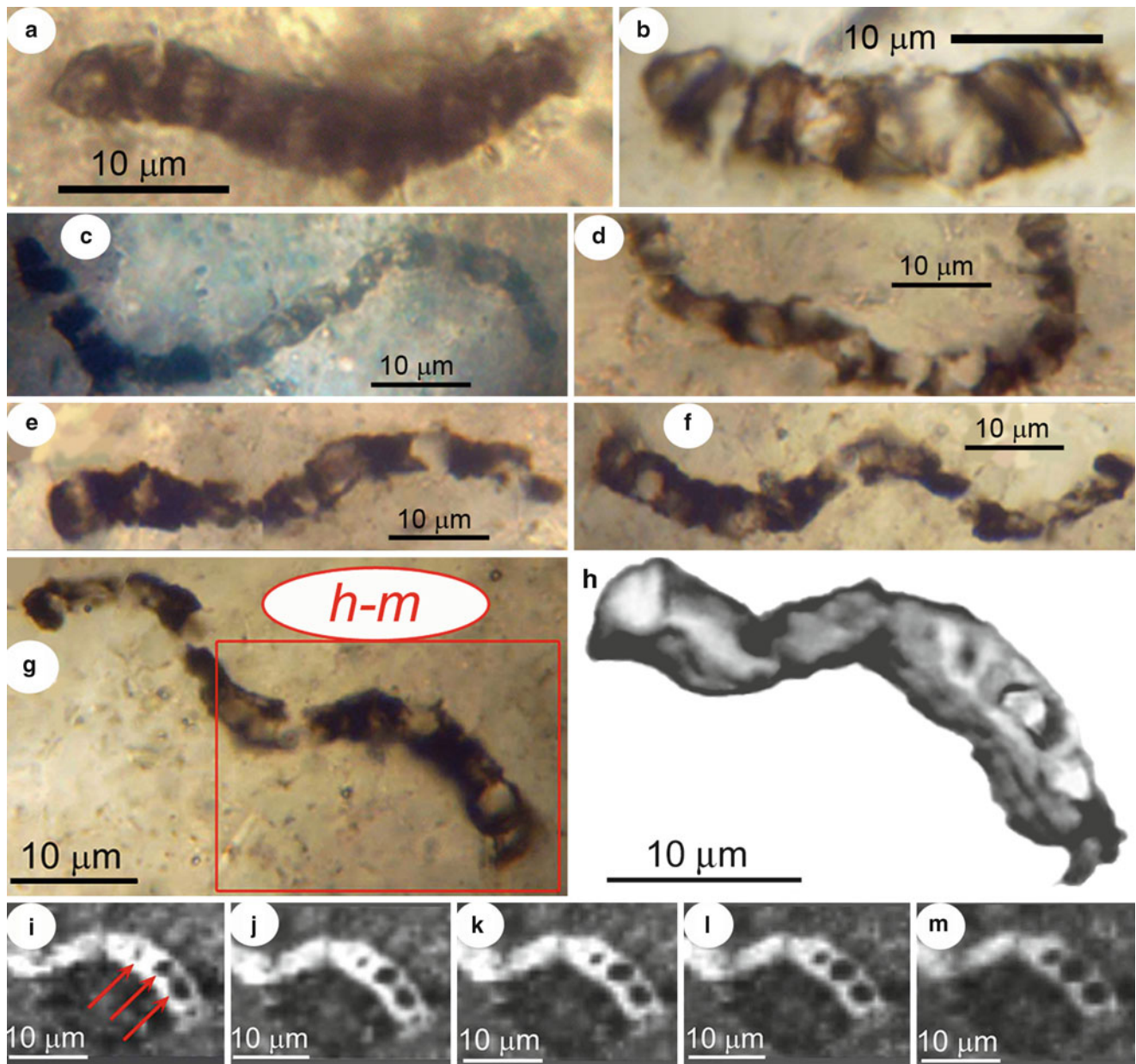
Fig. 2.9 Thin section-embedded filamentous bacteria *Incertae Sedis* (of uncertain systematic position) from the ~3,465-Ma-old Apex chert of northwestern Western Australia; all Raman images (**h** through **m**) were acquired in a spectral window centred in the kerogen "G" band at ~1,605 cm^{-1}. (**a**, **b**) Optical images of two specimens of *Primaevifilum conicoterminatum*, characterized by their discoidal medial cells and conical terminal cells. (**c**–**g**) Optical images of four specimens of *Primaevifilum amoenum*, in (**f**) and (**g**) showing two views of the same specimen situated 3–9 μm *below* the thin section surface; the *red rectangle* in (**g**) denotes the part of the filament shown in (**h**) through (**m**). (**h**) 3=D Raman image; the organic (carbonaceous, kerogenous) filament (*gray*) is cylindrical and, like younger Precambrian chert-embedded cellular fossils (Figs. 2.4b through h and p through x; 2.5b and c; 2.6a through i and h through u; 2.7b; and 2.8b, e and f), is composed of quartz-filled cells (*white*). (**i**–**m**) 2-D Raman images at sequential depths below the filament surface (**i**, at 0.75 μm; **j**, 1.5 μm; **k**, 2.25 μm; **l**, 3.0 μm; **m**, 3.75 μm); *arrows* in (**i**) point to quartz-filled cell lumina (*black*) defined by kerogenous cell walls (*white*), evident also in (**j** through **m**)

more recently been duplicated in studies of essentially the same suite of biomarkers extracted from multiple horizons of South African rock units ~2,600 Ma in age obtained from two boreholes geographically separated by some 24 km (Waldbauer et al. 2009).

Taken together, the available data indicate that sterane biomarkers date to ~2,700 Ma ago, well before the Great Oxidation Event of the early Proterozoic. As such, these biomarkers represent strong presumptive evidence of O$_2$-producing photoautotrophy during Archean Earth history.

2.6.2   Carbonaceous Kerogen

In contrast to extractable biomarkers, kerogen, the insoluble particulate organic matter of ancient sediments – whether in cherts or shales, and whether occurring as the carbonaceous constituents of cellularly preserved fossils, such as those illustrated here, or as finely divided dispersed coaly particles – is immobile, locked within its embedding rock matrix. In all carbonaceous rocks, whether Phanerozoic or Precambrian and whether or not they contain identifiable fossils, such kerogen occurs entirely or almost entirely as small particles of carbonaceous debris. Because this carbonaceous matter is demonstrably syngenetic with its encompassing mineral matrix, and because it comprises the great bulk of the carbonaceous components of ancient rocks, most analyses of Precambrian organic matter, and virtually all studies of Archean organic matter, have focused on the chemistry of kerogen. Three types of analyses have proved useful: (1) Raman spectroscopy of its molecular structure; (2) solid-state ^{13}C nuclear magnetic resonance (NMR) and X-ray absorption near-edge spectroscopy (XANES) studies of its elemental composition and functional groups; (3) mass spectrometric measurements of its carbon isotopic composition.

As shown in Figs. 2.4v through x and 2.9h through m, 2-D and 3-D Raman imagery provide firm evidence of the carbonaceous (kerogenous) composition of cellular preserved Precambrian microorganisms. Moreover, the Raman spectra on which such images are based can be analyzed to yield the Raman Index of Preservation (RIP) value of the kerogen that comprises the fossils (Schopf et al. 2005). These analyses provide an objective quantitative measure of the geochemical maturity (i.e. fidelity of preservation) of the fossilized organics that is of increasingly widespread use in palaeontology (e.g. Chen et al. 2007; Schopf et al. 2008, 2010; Schopf and Kudryavtsev 2009; Igisu et al. 2009). Thus, the oscillatoriacean trichome from the ~775-Ma-old Chichkan Formation shown in Fig. 2.4p through x has an RIP value of 8.6 (Schopf et al. 2010) indicating that it kerogenous components are only slightly more geochemically altered than those of the especially well-preserved Precambrian cyanobacteria from the ~800 Ma Bitter Springs Formation of central Australia shown in Figs. 2.4b, d, aa, 2.5b, c, and 2.6b through f and j (RIP = 9.0; Schopf et al. 2005). In contrast, the kerogenous cell walls of ~3,465-Ma-old filamentous fossil microbes from the Apex chert of northwestern Western Australia shown in Fig. 2.9a through m are geochemically more mature, having an RIP value of 5.0 (Schopf and Kudryavtsev 2009), but are decidedly less altered than the organic components of cyanobacteria preserved in many other Precambrian deposits (Schopf et al. 2005), such as the

highly graphitized stalk-forming pleurocapsaceans from the ~750-Ma-old River Wakefield Formation of South Australia shown in Fig. 2.8c through h (RIP = 1.0; Schopf et al. 2005). Although such data provide strong evidence of the biogenicity of the individual fossils analyzed (Schopf et al. 2008), they do not reveal their physiological characteristics.

Similarly, while studies using ^{13}C nuclear magnetic resonance and X-ray absorption near-edge spectroscopy have provided compelling evidence of the biological origin of the carbonaceous kerogen preserved in ~3,500-Ma-old deposits, they, too, are incapable of demonstrating the presence of O_2-producing cyanobacteria. Two recent publications illustrate the applicability of these techniques. Derenne et al. (2008) used ^{13}C NMR to analyze pyrolysates of kerogen isolated from the ~3,490-Ma-old Towers Formation of northwestern Western Australia by which they documented the presence of aliphatic carbon (CH_2 and CH_3), aromatic C=C (present in the polyaromatic hydrocarbons of which such kerogens are predominantly composed), and C-O and C=O functional groups, and demonstrated also the occurrence of an homologous series of long chain (C_{10}-C_{18}) aliphatic hydrocarbons exhibiting an odd-over-even carbon number predominance, "a unique characteristic of organics formed biologically since it reflects biosynthesis using addition of C2 units" (Derenne et al. 2008, p. 479). DeGregorio et al. (2009) used XANES, backed by other techniques, to establish the biological origin of kerogen in the ~3,465-Ma-old Apex chert, also of northwestern Western Australia and the source of the cellular filamentous Archean microbes illustrated in Fig. 2.9. Their comparative study of the Apex kerogen and that of the well-known microfossil-bearing ~1,900-Ma-old Gunflint chert of southern Ontario, Canada (Barghoorn and Tyler 1965; Cloud 1965), showed that the Apex kerogen contains functional groups – specifically, "carboxyl [–COOH] and phenol [$C_{aromatic}$-OH] peaks" – and that "Apex carbonaceous matter and Gunflint kerogen are chemically complex … [both containing] similar amounts of nitrogen, sulfur, and phosphorous [in which the presence of phosphorus, in particular] implies a biogenic origin" (DeGregorio et al. 2009, p. 632). Like two- and three-dimensional Raman imagery and the Raman spectral analyses discussed above, these studies establish "that the Apex microbe-like features represent authentic biogenic organic matter" (DeGregorio et al. 2009, p. 631) – an important conclusion that lays to rest the claim that the cellular fossils of the Apex chert and the organic matter of which they are composed are of non-biological origin (Brasier et al. 2002). Nevertheless, and again like the Raman data, even such detailed NMR and XANES analyses do not resolve the question of the Early Archean presence of oxygen-producing cyanobacteria.

2.6.3 Carbon Isotopic Evidence of Photosynthesis

Beginning with the pioneering studies of Park and Epstein (1963) and Hoering (1967), data have been amassed from thousands of analyses of the carbon isotopic compositions of inorganic carbonate minerals and carbonaceous kerogens coexisting in Precambrian sediments (e.g. Strauss and Moore 1992). Such data show a consistent difference between the inorganic and organic carbon analyzed in the relative abundances of the two stable isotopes of carbon, ^{12}C and ^{13}C, that extends from the present to ~3,500 Ma ago (Fig. 2.10).
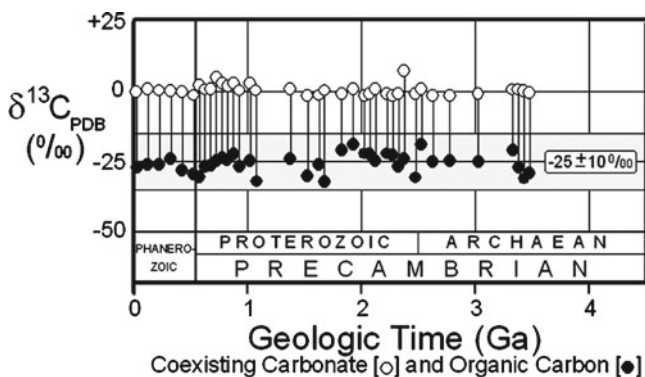

Fig. 2.10 Carbon isotopic values of coexisting carbonate and organic carbon measured in bulk samples of Phanerozoic and Precambrian sedimentary rocks, for the Precambrian represented by data from 100 fossiliferous cherts and shales shown as average values for groups of samples from 50-Ma-long intervals (Strauss and Moore 1992; Schopf 2004)

The enrichment of the fossil organic matter in the lighter isotope, ^{12}C, relative to coexisting carbonate (a proxy for the seawater-dissolved CO_2 required for its precipitation), and the magnitude of the isotopic difference (expressed as $\delta^{13}C_{PDB}$ values) between the inorganic and organic carbon reservoirs that invariably falls within a range of $\delta^{13}C_{PDB}$ values of $25 \pm 10‰$, are consistent with the carbon isotopic fractionation that occurs as a result of Rubisco- (ribulose bis-phospate carboxylase/oxygenase-) mediated CO_2-fixation in O_2-producing cyanobacteria (e.g. Hayes et al. 1983, 1992; House et al. 2000, 2003). Such evidence of carbon isotopic fractionation is well documented in rocks ~3,200 to ~3,500 Ma, the oldest fossil-bearing deposits known (Fig. 2.11).

Despite this strong continuous carbon isotopic evidence of photosynthesis, dating to ~3,500 Ma ago, it does not necessarily reflect the Archean presence of cyanobacteria. Because of the mixing of carbonaceous matter from diverse biological sources that occurs as sediments are deposited and the alteration of carbon isotopic compositions that can occur during geological metamorphism, the $\delta^{13}C_{PDB}$ values of the analyzed kerogen range broadly ($\pm 10‰$) and, thus, are consistent not only with primary production by cyanobacteria but by non-O_2-producing photosynthetic bacteria as well. Archean kerogens may have been derived from either or both of these sources. Moreover, interpretation of the data is complicated by the presence in Archean sediments of carbonaceous matter so enriched in ^{12}C as to be plausibly derived only from CH_4-metabolizing methanotrophs, indicating that methane-producing Archaea played a significant role in the ancient ecosystem (Hayes 1983; Schopf 1994b). [As an
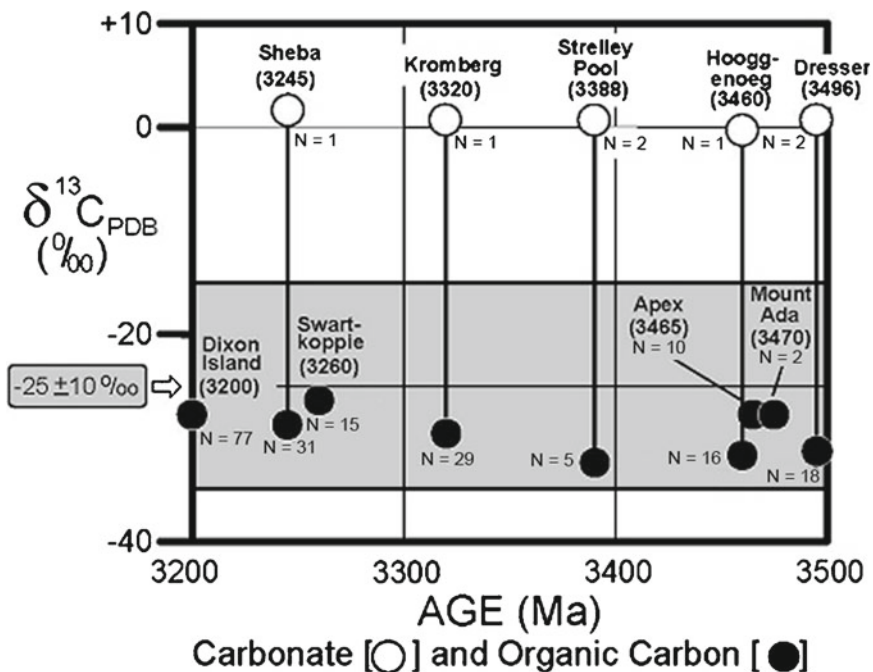

Fig. 2.11 Carbon isotopic values of carbonate and organic carbon measured in bulk samples of nine of the oldest microfossiliferous units known (Schopf 2006)

aside, it should be noted that isotopic analyses of sedimentary pyrite (FeS_2), enriched in S^{32} due to microbial activity, indicate that that sulphate-reducing bacteria were also present in Earth's early biota (Schopf 1999, 2009) and that the presence of ^{12}C-rich graphitic carbon in the oldest sedimentary rocks now known, from Akilia Island off southwestern Greenland, suggests that photosynthetic microbes may have existed as early as ~3,830 million years ago (McKeegan et al. 2007).]

2.7 Conclusions

Microbial communities composed of members of diverse prokaryotic lineages have been extant since early in Earth history (Fig. 2.12). Among such microbes, the most abundant and best documented are cyanobacteria, represented by members of five families: Oscillatoriaceae, Nostocaceae, Chroococcaceae, Entophysalidaceae, Pleurocapsaceae. Perhaps the most striking aspect of the cyanobacterial fossil record is the large body of evidence that documents the evolutionary stasis of diverse members of the group over vast segments of geological time. Such stasis may, or may not be characteristic of microbial lineages generally, but for cyanobacteria it is established firmly by the essentially identical morphologies, life cycles, and ecologic settings exhibited by cyanobacterial fossils and their modern counterparts. In this regard, and despite the fact that cyanobacterial fossils are now known from hundreds of ancient geological units, it is important to note that active studies of the fossil record of the group are of relatively recent vintage and that the documented cyanobacterial fossil record pales in comparison with that of many animal lineages such as trilobites, ammonites, corals, clams, brachiopods, fossils of which have been collected and catalogued for more than two centuries. While much more evidence would be needed to sort out rapid evolution like that typical of eukaryotic plants and animals, even the relatively depauperate cyanobacterial fossil record now known is sufficient to show *lack* of change, maintenance of an evolutionary status quo, over geologically vast periods.

Given the evidence currently available, the times of origin of the various cyanobacterial families can be estimated only approximately (Fig. 2.12) from geological records. Not only is their known fossil record limited by the fact that studies are relatively recent, but their preservation in the rock record, whether as permineralized (petrified) cells in cherty stromatolites or as compressed carbonaceous remnants in shales or siltstones, requires unusual conditions. Moreover, even for more readily preservable organisms such as shelled invertebrate animals the oldest *detected* occurrence of a given lineage is certain to be younger (and for cyanobacteria, perhaps very much younger) than first *actual* occurrences. For truly ancient organisms like cyanobacteria this problem is compounded by the incompleteness of the surviving, potentially fossil-bearing rock record, which becomes increasingly sparse and patchy in units older than ~2,000 Ma, a deficiency particularly acute for rocks of Archean-age (>2,500-Ma-old), which comprise only a miniscule percentage of deposits that have survived to the present. Yet here, too, the available data are sufficient to establish that microbial communities were extant and flourishing early in Earth history: microbially produced stromatolites are known from
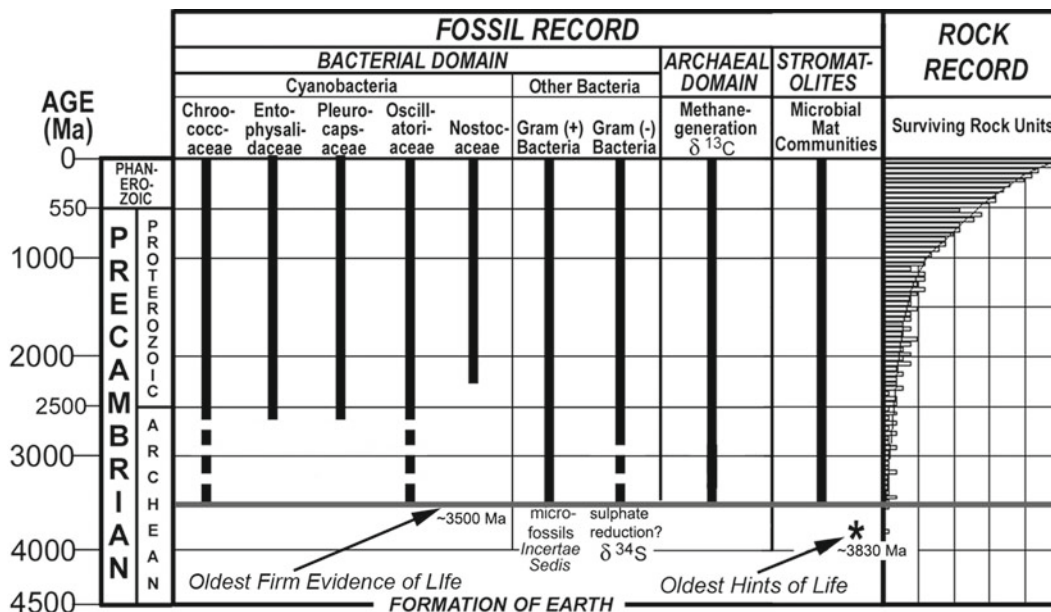

Fig. 2.12 The known fossil record of Bacteria, Archaea, microbially laminated stromatolites, and surviving rock units over geological time, indicating that the oldest firm evidence of life dates from ~3,500 Ma, whereas hints of life are known from rocks ~3,830 Ma in age

48 Archean geological units, of which ten date from between 3,200 and 3,500 Ma ago (Fig. 2.2). *Bona fide* microfossils, comprising six broad bacterium-like morphotypes, have been reported from 40 Archean rock units, of which 14 date from the interval between 3,200 and 3,500 Ma ago (Schopf 2006). Organic geochemical evidence in the form of sterane biomarkers in ~2,700-Ma-old rocks and biogenic carbonaceous kerogen and carbon isotopic evidence in rocks dating to ~3,500 Ma ago well document the presence of microbe-level life early in Earth history. Taken as a whole, the evidence indicates that O_2-producing cyanobacteria originated earlier than the Great Oxidation Event at ~2,450 Ma ago; that such microbes were extant by 2,700 Ma ago; and that the origin of oxygenic photosynthesis may date from as early as, or even earlier than, 3,500 Ma ago.

Regardless of their time of origin, the early evolutionary success of cyanobacteria can be attributed to their photosynthetic production of gaseous oxygen, a toxin lethal to the earlier-evolved strictly anaerobic photosynthetic bacteria with which they initially competed for photosynthetic space (Schopf 1999). Once established, their evolutionary stasis (hypobradytelic rate of evolution; Schopf 1994a) was in part a result of their microscopic size and correspondingly huge populations, their ease of global distribution (by water currents, winds, hurricanes and the like), and their asexual reproduction and the lack of genetic variability it provides. The root of such stasis, however, seems almost certainly to lie in their exceptional ecologic tolerance (Schopf 1994a). Over their exceedingly long evolutionary history, cyanobacteria adapted to the slowly changing global environment – from anoxic to oxygenic, UV-rich to UV-deficient, CO_2-rich to CO_2-deficient, short to increasingly longer day-lengths and, perhaps, from relatively high ambient temperatures (~60°C) to that of the present-day Earth (~15°C). The genomes of cyanobacteria thus encode a history of adaptation unparalleled by virtually any other group of organisms. Throughout their remarkably long-term existence, prokaryotic cyanobacteria have survived and thrived to rank among the most successful forms of life ever to have emerged in life's long history.

References

Allwood AC, Walter MR, Kamber BS, Marshall CP, Burch IW (2006) Stromatolite reef from the Early Archaean era of Australia. Nature 441:714–718

Altermann W, Schopf JW (1995) Microfossils from the Neoarchean Campbell Group, Griqualand West Sequence of the Transvaal Supergroup, and their paleoenvironmental and evolutionary implications. Precambrian Res 75:65–90

Barghoorn ES, Schopf JW (1965) Microorganisms from the late Precambrian of central Australia. Science 150:337–339

Barghoorn ES, Tyler SA (1965) Microorganisms from the Gunflint chert. Science 147:563–577

Blankenship RE (1992) Origin and early evolution of photosynthesis. Photosynth Res 33:91–111

Blankenship RE, Hartman H (1998) The origin and evolution of oxygenic photosynthesis. Trends Biochem Sci 23:94–97

Bloeser B (1985) *Melanocyrillium*, a new genus of structurally complex late Proterozoic microfossils from the Kwagunt Formation (Chuar Group), Grand Canyon, Arizona. J Paleontol 59:741–765

Bloeser B, Schopf JW, Horodyski RJ, Breed WJ (1977) Chitinozoans from the late Precambrian Chuar Group of the Grand Canyon, Arizona. Science 195:676–679

Brasier MD, Green OR, Jephcoat AP, Kleppe AK, VanKranendonk AJ, Lindsay JF, Steele A, Grassineau NV (2002) Questioning the evidence of Earth's oldest fossils. Nature 416:76–81

Brocks JJ, Logan GA, Buick R, Summons RE (1999) Archean molecular fossils and the early rise of eukaryotes. Science 285:1033–1036

Butterfield NJ (2009) Modes of pre-Ediacaran multicellularity. Precambrian Res 173:201–211

Canfield DE (2005) The early history of atmospheric oxygen: homage to Robert M. Garrels. Annu Rev Earth Planet Sci 33:1–36

Chen JY, Schopf JW, Bottjer DJ, Zhang C-Y, Kudryavtsev AB, Tripathi AB, Wang X-Q, Yang Y-H, Gao X, Yang Y (2007) Raman spectra of a ctenophore embryo from southwestern Shaanxi, China. Proc Natl Acad Sci USA 104:6289–6292

Cloud PE (1965) Significance of the Gunflint (Precambrian) microflora. Science 148:27–45

Darwin CR (1859) On the origin of species by means of natural selection. John Murray, London, 490 pp

DeGregorio BT, Sharp TG, Flynn GJ, Wirick S, Hervig RL (2009) Biogenic origin for Earth's oldest putative fossils. Geology 37:631–634

Derenne S, Robert F, Skrzypczak-Bonduelle A, Gourier D, Binet L, Rouzaud J-N (2008) Molecular evidence for life in the 3.5 billion year old Warrawoona chert. Earth Planet Sci Lett 272:476–480

Drews G (1973) Fine structure and chemical composition of the cell envelopes. In: Carr NG, Whitton BA (eds) The biology of blue-green algae. Blackwell Scientific Publications/University of California Press, Oxford/Berkeley, pp 99–116, 676 pp

Eigenbrode JL, Freeman KH, Summons RE (2008) Methylhopane biomarker hydrocarbons in Hamersley Province sediments provide evidence for Neoarchean aerobiosis. Earth Planet Sci Lett 273:323–331

Fairchild TR (1975) The geologic setting and paleobiology of a Late Precambrian stromatolitic microflora from South Australia. Dissertation, University of California, Los Angeles, 272 pp

Farquhar J, Bao H, Thiemens M (2000) Atmospheric influence of Earth's earliest sulfur cycle. Science 289:756–759

Farquhar J, Peterson M, Johnson DT, Strauss H, Masterson A, Weichert U, Kaufman AJ (2007) Isotopic evidence for Mesoarchaean anoxia and changing atmospheric sulfur chemistry. Nature 449:706–709

Frank H, Lefort M, Martin HH (1971) Elektronenoptische und chemische Untersuchungen an Zellwänden der Blaualgen, *Phormidium unicinatum*. Z Natur B 17:262–268

Garrels RM, Mackenzie FT (1971) Evolution of sedimentary rocks. Norton, New York, 397 pp

Giovannoni SJ, Turner S, Olsen GJ, Barns S, Lane DJ, Pace NR (1988) Evolutionary relationship among cyanobacteria and green chloroplasts. J Bacteriol 170:3584–3592

Golubić S, Hofmann HJ (1976) Comparison of Holocene and mid-Precambrian Entophysalidaceae (Cyanophyta) in stromatolitic mats: cell division and degradation. J Paleontol 50:1074–1082

Golubić S, Sergeev VN, Knoll AH (1995) Mesoproterozoic *Archaeoellipsoides*: akinetes of heterocystous cyanobacteria. Lethaia 28:285–298

Green JW, Knoll AH, Golubić S, Swett K (1987) Paleobiology of distinctive benthic microfossils from the Upper Proterozoic Limestone-Dolomite "Series," central East Greenland. Am J Bot 74:928–940

Green JW, Knoll AH, Swett K (1988) Microfossils from oolites and pisolites of the Upper Proterozoic Eleonore Bay Group, central East Greenland. J Paleontol 62:835–852

Grotzinger JP, Knoll AH (1999) Stromatolites in Precambrian carbonates: evolutionary mileposts or environmental dipsticks? Annu Rev Earth Planet Sci 27:313–358

Halfen LN, Castenholz RW (1971) Gliding motility in the blue-green alga, *Oscillatoria princeps*. J Phycol 7:133–145

Hayes JM (1983) Geochemical evidence bearing on the origin of aerobiosis, a speculative hypothesis. In: Schopf JW (ed) Earth's earliest biosphere, its origin and evolution. Princeton University Press, Princeton, pp 291–301, 543 pp

Hayes JM, Kaplan IR, Wedeking KM (1983) Precambrian organic geochemistry, preservation of the record. In: Schopf JW (ed) Earth's earliest biosphere, its origin and evolution. Princeton University Press, Princeton, pp 93–134, 543 pp

Hayes JM, DesMarais DJ, Lambert IA, Strauss H, Summons RE (1992) Proterozoic biogeochemistry. In: Schopf JW, Klein C (eds) The Proterozoic biosphere, a multidisciplinary study. Cambridge University Press, New York, pp 81–134, 1348 pp

Herdman M, Janvier M, Rippka R, Stanier RY (1979a) Genome size of cyanobacteria. J Gen Microbiol 111:73–85

Herdman M, Janvier M, Waterbury JB, Rippka R, Stanier RY, Mandel M (1979b) Deoxyribonucleic acid base composition of cyanobacteria. J Gen Microbiol 111:63–71

Hoering TC (1967) The organic geochemistry of Precambrian rocks. In: Abelson PH (ed) Researches in geochemistry, vol 2. Wiley, New York, pp 87–111, 663 pp

Hofmann HJ (1976) Precambrian microflora, Belcher Islands, Canada: significance and systematics. J Paleontol 50:1040–1073

Hofmann HJ (2000) Archean stromatolites as microbial archives. In: Riding RE, Awramik SM (eds) Microbial sediments. Springer, Berlin/Heidelberg/New York, pp 315–327, 331 pp

Hofmann HJ, Grey K, Hickman AH, Thorpe RI (1999) Origin of 3.45 Ga conform stromatolites in Warrawoona Group, Western Australia. Geol Soc Am Bull 111:1256–1262

Holland HD (2002) Volcanic gases, black smokers, and the Great Oxidation Event. Geochim Cosmochim Acta 66:3811–3826

Horodyski RJ, Donaldson JA (1980) Microfossils from the Middle Proterozoic Dismal Lakes Group, Arctic Canada. Precambrian Res 11:125–159

House CH, Schopf JW, McKeegan KD, Coath CD, Harrison TM, Stetter KO (2000) Carbon isotopic composition of individual Precambrian microfossils. Geology 28:707–710

House CH, Schopf JW, Stetter KO (2003) Carbon isotopic signatures of biochemistry: fractionation by archaeans and other thermophilic prokaryotes. Org Geochem 34:345–356

Igisu M, Ueno Y, Shimojima M, Nakashima S, Awramik SM, Ohta H, Maryuama S (2009) Micro-FTIR spectroscopic signatures of bacterial lipids in Proterozoic microfossils. Precambrian Res 173:19–26

Kidston R, Lang WH (1922) On Old Red Sandstone plants showing structure from the Rhynie chert bed, Aberdeenshire, part V. Trans R Soc Edinb 52:885–902

Knoll AH, Barghoorn ES, Golubić S (1975) *Palaeopleurocapsa wopfnerii* gen. et sp nov., a late-Precambrian blue-green alga and its modern counterpart. Proc Natl Acad Sci USA 72:2488–2492

Knoll AH, Golubić S, Green J, Swett K (1986) Organically preserved microbial endoliths from the late Proterozoic of East Greenland. Nature 321:856–857

McKeegan KD, Kudryavtsev AB, Schopf JW (2007) Raman and ion microscopic imagery of graphite inclusions in apatite from older than 3830 Ma Akilia supracrustal rocks, west Greenland. Geology 35:591–594

Mojzsis S, Arrenhius G, McKeegan KD, Nutman AP, Friend CRL (1996) Evidence for life on Earth before 3,800 million years ago. Nature 384:55–59

Oparin AI (1938) The origin of life. McMillian, New York, 270 pp

Pankratz HS, Bowen CC (1963) Cytology of blue-green algae. I. The cells of Symploca muscorum. Am J Bot 50:387–399

Park R, Epstein S (1963) Carbon isotopic fractionation during photosynthesis. Geochim Cosmochim Acta 21:110–115

Porter SM, Knoll AH (2000) Testate amoebae in the Neoproterozoic Era: evidence from vase-shaped microfossils in the Chuar Group, Grand Canyon. Paleobiology 26:360–385

Rasmussen B, Fletcher IR, Brocks JJ, Kilburn MR (2008) Reassessing the first appearance of eukaryotes and cyanobacteria. Nature 455:1101–1104

Rippka R, Deruelles J, Waterbury JB, Herdman M, Stanier RY (1979) Generic assignments, strain histories and properties of pure cultures of cyanobacteria. J Gen Microbiol 111:1–61

Schopf JW (1968) Microflora of the bitter springs formation, late Precambrian, central Australia. J Paleontol 42:651–688

Schopf JW (1977) Biostratigraphic usefulness of stromatolitic Precambrian microbiotas: a preliminary analysis. Precambrian Res 5:143–173

Schopf JW (1978) The evolution of the earliest cells. Sci Am 239:110–138

Schopf JW (1992a) Paleobiology of the Archean. In: Schopf JW, Klein C (eds) The Proterozoic biosphere, a multidisciplinary study. Cambridge University Press, New York, pp 25–39, 1348 pp

Schopf JW (1992b) Proterozoic prokaryotes: affinities, geologic distribution, and evolutionary trends. In: Schopf JW, Klein C (eds) The Proterozoic biosphere, a multidisciplinary study. Cambridge University Press, New York, pp 195–218, 1348 pp

Schopf JW (1992c) Evolution of the Proterozoic biosphere: benchmarks, tempo, and mode. In: Schopf JW, Klein C (eds) The Proterozoic biosphere, a multidisciplinary study. Cambridge University Press, New York, pp 583–600, 1348 pp

Schopf JW (1993) Microfossils of the Early Archean Apex chert: new evidence of the antiquity of life. Science 260:640–646

Schopf JW (1994a) Disparate rates, differing fates: the rules of evolution changed from the Precambrian to the Phanerozoic. Proc Natl Acad Sci USA 91:6735–6742

Schopf JW (1994b) The oldest known records of life: stromatolites, microfossils, and organic matter from the Early Archean of South Africa and Western Australia. In: Bengtson S (ed) Early life on earth. Columbia University Press, New York, pp 193–206, 656 pp

Schopf JW (1996) Metabolic memories of Earth's earliest biosphere. In: Marshall CR, Schopf JW (eds) Evolution and the molecular revolution. Jones and Bartlett, Boston, pp 73–105

Schopf JW (1999) Cradle of life, the discovery of earth's earliest fossils. Princeton University Press, Princeton, 367 pp

Schopf JW (2004) Geochemical and submicron-scale morphologic analyses of individual Precambrian microorganisms. In: Hill JR, Aizenshtat Z, Baedecker MJ, Claypool G, Eganhouse R, Goldhaber M, Leventhal J, Peters K (eds) Geochemical investigation in Earth and Space Science: a tribute to Isaac R. Kaplan. The Geochemical Society, St. Louis, pp 365–375, 466 pp

Schopf JW (2006) Fossil evidence of Archaean life. Philos Trans R Soc B 361:869–885

Schopf JW (2009) Paleontology, microbial. In: Lederberg J, Schaechter M (eds) Encyclopedia of microbiology, 3rd edn. Elsevier, Amsterdam, pp 390–400, 4600 pp

Schopf JW, Bottjer DJ (2009) Preface: world summit on ancient microscopic fossils. Precambrian Res 173:1–3

Schopf JW, Kudryavtsev AB (2005) Three-dimensional Raman imagery of Precambrian microscopic organisms. Geobiology 3:1–12

Schopf JW, Kudryavtsev AB (2009) Confocal laser scanning microscopy and Raman imagery of ancient microscopic fossils. Precambrian Res 173:9–49

Schopf JW, Kudryavtsev AB, Agresti DG, Wdowiak TJ, Czaja AD (2002) Laser-Raman imagery of Earth's earliest fossils. Nature 416:73–76

Schopf JW, Kudryavtsev AB, Agresti DG, Czaja AD, Wdowiak TJ (2005) Raman imagery: a new approach to assess the geochemical maturity and biogenicity of permineralized Precambrian fossils. Astrobiology 5:333–371

Schopf JW, Tripathi AB, Kudryavtsev AB (2006) Three-dimensional optical confocal imagery of Precambrian microscopic organisms. Astrobiology 1:1–16

Schopf JW, Kudryavtsev AB, Czaja AD, Tripathi AB (2007) Evidence of Archean life: stromatolites and microfossils. Precambrian Res 158:141–155

Schopf JW, Tewari VC, Kudryavtsev AB (2008) Discovery of a new chert-permineralized microbiota of the Proterozoic Buxa Formation of the Ranjit Window, Sikkim, N.E. India, and its astrobiological implications. Astrobiology 8:735–746

Schopf JW, Kudryavtsev AB, Sergeev VN (2010) Confocal laser scanning microscopy and Raman imagery of the Late Neoproterozoic Chichkan microbiota of South Kazakhstan. J Paleontol 84:402–416

Strauss H, Moore TB (1992) Abundances and isotopic compositions of carbon and sulfur species in whole rock and kerogen samples. In: Schopf JW, Klein C (eds) The Proterozoic biosphere, a multidisciplinary study. Cambridge University Press, New York, pp 709–798, 1348 pp

Summons RE (1992) Abundance and composition of extractable organic matter. In: Schopf JW, Klein C (eds) The Proterozoic biosphere, a multidisciplinary study. Cambridge University Press, New York, pp 101–115, 1348 pp

Summons RE, Bradley AS, Janke LL, Waldbauer JR (2006) Steroids, triterpenoids and molecular oxygen. Philos Trans R Soc B 361:951–968

Waldbauer JR, Sherman LS, Sumner DY, Summons RE (2009) Late Archean molecular fossils from the Transvaal Supergroup record the antiquity of microbial diversity and aerobiosis. Precambrian Res 169:28–47

Zehr JP, Mellon TM, Hiorns WH (1997) Phylogeny of cyanobacterial nifH genes: evolutionary implications and potential applications to natural assemblages. Microbiology 143:1443–1450

Zhang Y, Golubić S (1987) Endolithic microfossils (Cyanophyta) from Early Proterozoic stromatolites, Hebei, China. Acta Micropaleontol Sin 4:1–12